nature biotechnology

Article

https://doi.org/10.1038/s41587-023-01779-8

A highly efficient transgene knock-in technology in clinically relevant cell types

Received: 19 August 2022

Accepted: 4 April 2023

Published online: 01 May 2023

Check for updates

Alexander G. Allen[1,2], Samia Q. Khan[1,2], Carrie M. Margulies[1,2], Ramya Viswanathan[1,2], Swarali Lele[1], Laura Blaha[1], Sean N. Scott[1], Kaitlyn M. Izzo[1], Alexandra Gerew[1], Rithu Pattali[1], Nadire R. Cochran[1], Carl S. Holland[1], Amy H. Zhao[1], Stephen E. Sherman[1], Michael C. Jaskolka[1], Meng Wu[1], Aaron C. Wilson[1], Xiaoqi Sun[1], Dawn M. Ciulla[1], Deric Zhang[1], Jacqueline D. Nelson[1], Peisheng Zhang[1], Patrizia Mazzucato[1], Yan Huang[1], Georgia Giannoukos[1], Eugenio Marco[1], Michael Nehil[1], John A. Follit[1], Kai-Hsin Chang[1], Mark S. Shearman[1], Christopher J. Wilson[1] & John A. Zuris[1]

Inefficient knock-in of transgene cargos limits the potential of cell-based medicines. In this study, we used a CRISPR nuclease that targets a site within an exon of an essential gene and designed a cargo template so that correct knock-in would retain essential gene function while also integrating the transgene(s) of interest. Cells with non-productive insertions and deletions would undergo negative selection. This technology, called SLEEK (SeLection by Essential-gene Exon Knock-in), achieved knock-in efficiencies of more than 90% in clinically relevant cell types without impacting long-term viability or expansion. SLEEK knock-in rates in T cells are more efficient than state-of-the-art *TRAC* knock-in with AAV6 and surpass more than 90% efficiency even with non-viral DNA cargos. As a clinical application, natural killer cells generated from induced pluripotent stem cells containing SLEEK knock-in of CD16 and mbIL-15 show substantially improved tumor killing and persistence in vivo.

Cell-based medicines have enabled substantial progress in addressing serious diseases spanning cancer[1], autoimmune disorders[2] and hemoglobinopathies[3]. In cancer immunotherapy, autologous T cells with an integrated chimeric antigen receptor (CAR) have transformed treatment for hematopoietic malignancies bearing CD19 or B cell maturation antigen (BCMA) surface antigens[4–6]. Other engineered immune cells, such as natural killer (NK) cells, also show promise for cancer immunotherapy[1], with genomic insertions of functional cargos such as CARs[7,8] to target tumor antigens, CD16 to improve antibody-dependent cellular cytotoxicity (ADCC)[9–12] and a version of membrane-bound interleukin-15 (mbIL-15) to improve persistence[13–16].

Genomic insertion of transgene cargos into cells has improved in recent years. The field has moved from random integration with gamma retroviral and lentiviral vectors to targeted, site-specific insertion methods using gene editing technologies such as CRISPR–Cas[17]. Nonetheless, considerable challenges remain[10]. Adeno-associated virus serotype 6 (AAV6) is the most efficient DNA cargo format for knock-in (KI) into primary hematopoietic cells[17–19]; however, the cost and time associated with Good Manufacturing Practice (GMP) AAV manufacture is considerable, and the packaging capacity is limited to <4.7 kilobases (kb)[20]. Additionally, the rates of KI are often capped around 60–70% in the most amenable cell types, despite major efforts to improve homology-directed repair (HDR) efficiency[19]. The principal challenge to achieving near 100% CRISPR–Cas-based KI across cell types is that cells have a strong preference to repair nuclease-induced double-strand breaks (DSBs) through non-homologous end joining

[1]Editas Medicine, Cambridge, MA, USA. [2]These authors contributed equally: Alexander G. Allen, Samia Q. Khan, Carrie M. Margulies, Ramya Viswanathan. e-mail: john.zuris@editasmed.com

(NHEJ) rather than HDR[21]. To overcome this challenge, we designed a technology called SLEEK (SeLection by Essential-gene Exon Knock-in) that selects for HDR-mediated KI and against NHEJ-mediated insertions and deletions (indels) while also guaranteeing high-level constitutive expression of the transgene cargo. SLEEK combines CRISPR–Cas editing of an essential gene with a DNA KI template that restores the essential gene coding sequence while incorporating the transgene cargo. Indels that lead to disruption of an essential protein are lethal. For this approach to work efficiently, editing rates must approach 100% to limit the presence of unedited cells. Additionally, the promoter of the essential gene can be leveraged to achieve high-level constitutive gene expression of the transgene, with limited possibility of silencing, which is a major concern when generating cell therapies from induced pluripotent stem cells (iPSCs)[22].

Using SLEEK, we demonstrate bulk KI efficiencies of more than 90% in iPSCs using a plasmid DNA template and between 85% and 95% in B cells, T cells and NK cells using AAV6 DNA templates. We show this with several clinically important cargos, achieving these high efficiencies with both viral and non-viral DNA templates. We further show that it is possible to tune cargo expression by KI at different essential genes bearing different endogenous promoter strengths. To demonstrate the utility of SLEEK for generating iPSC-derived NK (iNK) cells for the treatment of solid tumors, we knocked-in CD16 and mbIL-15 into iPSCs at the glyceraldehyde-3-phosphate dehydrogenase (*GAPDH*) locus. These CD16-mbIL-15 double knock-in (SLEEK DKI) iPSCs were then differentiated into iNKs where they showed a substantial increase in tumor killing and persistence both in vitro and in vivo. We observed undetectable tumor burden in an animal model after treatment with SLEEK DKI iNK cells and demonstrated improved iNK in vivo persistence, which we attribute to the robust expression of both transgene cargos driven by the strong endogenous *GAPDH* promoter. Taken together, this work demonstrates that SLEEK can be used for incorporation of multiple transgene cargos that are needed for the next generation of engineered cell-based medicines.

Results

SLEEK leads to high efficiency of transgene cargo insertion

To test the feasibility of SLEEK (Fig. 1a), the *GAPDH* locus was selected because *GAPDH* is an essential gene and resistant to promoter silencing[22]. We screened guide RNAs (gRNAs) in the *GAPDH* last exon with a high-activity engineered AsCas12a nuclease[19] and identified several gRNA and ribonucleoprotein (RNP) combinations, referred to as SLEEK gRNA and SLEEK RNP, respectively. DNA KI templates were designed such that accurate integration would create a DNA sequence restoring expression of a full-length GAPDH protein followed by a ribosomal skipping P2A peptide[23] and one or more transgene cargos of interest (Fig. 1b). Upon editing with SLEEK RNP and a circular plasmid DNA template in iPSCs, we initially observed low cargo KI efficiency as measured by flow cytometry after 2 days (Fig. 1c). Within 1 week, however, the percentage of cells with green fluorescent protein (GFP) cargo increased from 11% to 93% (Fig. 1c and Supplementary Fig. 1a). Fluorescent microscopy images taken over 9 days confirmed selection of GFP$^+$ SLEEK KI cells (Fig. 1b). SLEEK KI was further confirmed by droplet digital polymerase chain reaction (ddPCR) (Supplementary Fig. 1b). We verified the hypothesized SLEEK mechanism of action by assessing KI efficiency when instead targeting an intron region in *GAPDH* just upstream of the identified SLEEK gRNA. The two AsCas12a RNPs each generated indels at more than 95% efficiency after 48 h (Supplementary Fig. 1c). However, when KI cassettes were designed in similar formats for both sites (Supplementary Fig. 1d), we saw substantially lower KI rates at the intron target site at 2.1% compared to the exon target site at 95.6% (Supplementary Fig. 1e), supporting our hypothesis that SLEEK works by restoring an otherwise lethal indel in an essential gene, which, for *GAPDH*, is found in the last exon site but not in the intron site. Because SLEEK leverages indel creation at essential gene alleles to negatively select for cells lacking KI into the *GAPDH* allele, we next wanted to assess whether healthy iPSC clones could be isolated with both mono-allelic or bi-allelic KI of the GFP cargo. We performed SLEEK and plated single-cell clones for eventual genotypic analysis by ddPCR and RNase H2-dependent amplicon sequencing (rhAmpSeq) analysis[24]. We confirmed that both heterozygous and homozygous SLEEK KI iPSC clones could be isolated (Supplementary Fig. 1f). We found that heterozygous SLEEK KI clones predominantly contained a disrupting indel in the other *GAPDH* allele, indicating that a single functional copy of *GAPDH* is sufficient for cell survival (Supplementary Fig. 1g).

SLEEK is compatible with other CRISPR nucleases and DNA template formats

The design of SLEEK constructs and SLEEK site selection are important to achieve optimal performance and can be extended to other nucleases. For SLEEK HDR to be successful, we designed the recoded exon such that the cell repair machinery would not use the last exon sequence in the KI cassette as the 3′ homology arm, as this would enable restoration of GAPDH protein function but without insertion of the transgene cargo (Supplementary Fig. 2a). To ensure that the SLEEK KI cassette 3′ homology arm was used as the template for HDR, we modified the maximal number of DNA nucleotides in the protein-coding region of the recoded last exon without changing the GAPDH amino acid sequence (Supplementary Fig. 2a). The SLEEK selection mechanism works particularly well at a specific site in *GAPDH* where the SLEEK RNP targets an asparagine (N316) residue critical for GAPDH protein function[25]. Based on indel patterns that we measured by next-generation sequencing (NGS), the vast majority of indels, whether in-frame or not, ended up being deleterious in the absence of a supporting allele containing the in-frame SLEEK KI cargo with the restored last exon (Supplementary Fig. 2b). Finally, we tested whether SLEEK would work with other nucleases such as SpCas9 (Supplementary Fig. 2c), and, after testing several guides that target at or near the AsCas12a *GAPDH* SLEEK site, we identified an SpCas9 guide capable of achieving up to 99.0% SLEEK KI in iPSCs (Supplementary Fig. 2c,d).

Fig. 1 | SLEEK achieves the highest transgene cargo KI efficiency currently in the field. a, Overview of SLEEK concept based on selection for KI, or HDR edits, over those that create lethal NHEJ-mediated indel edits, in an essential gene. **b**, SLEEK schematic at molecular level showing how restoration of recoded last exon contained within the DNA template is key for making a functional GAPDH protein and that cell survival is dependent on correct in-frame integration into the locus of this essential gene. Asterisk is the stop codon. Not drawn to scale. **c**, Timecourse to assess GFP KI efficiency in iPSCs using SLEEK over 9 days by flow cytometry, including flow cytometry plot of unedited cells on day 9. Fluorescent microscopy images assessing GFP expression in edited iPSCs at 3 days and 9 days after editing are also shown; scale bar is 500 µm. **d**, Assessment of GFP SLEEK KI efficiency with several different DNA templates in human iPSCs. $n = 3$ independent experiments; line represents mean; $^{****}P < 0.0001$, analyzed using one-way ANOVA followed by Bonferroni's multiple comparisons test. **e**, Two additional SLEEK target genes, *TBP* and *KIF11*, selected both because they are essential to survival and because their endogenous expression levels are known to be different from *GAPDH*, were assessed for SLEEK GFP KI efficiency by flow cytometry both for percent positive cells, denoted by percentage, and for MFI of GFP signal. Plasmid: circular dsDNA cassette containing SLEEK KI cassette and kanamycin resistance gene marker and other bacterial plasmid components. Linear ssDNA: ssDNA containing only SLEEK cargo and homology arm sequence. Linear dsDNA: linear dsDNA sequence containing only SLEEK KI cargo and homology arms. Closed-ended dsDNA: dsDNA containing only SLEEK KI cargo and homology arms protected on both ends by a closed loop of ssDNA. Marker-free plasmid: circular dsDNA plasmid containing only KI cassette and minimal additional DNA sequence, such as restriction sites needed for linearization. CDS, coding sequence; SSC, side scatter.

https://doi.org/10.1038/s41587-023-01779-8

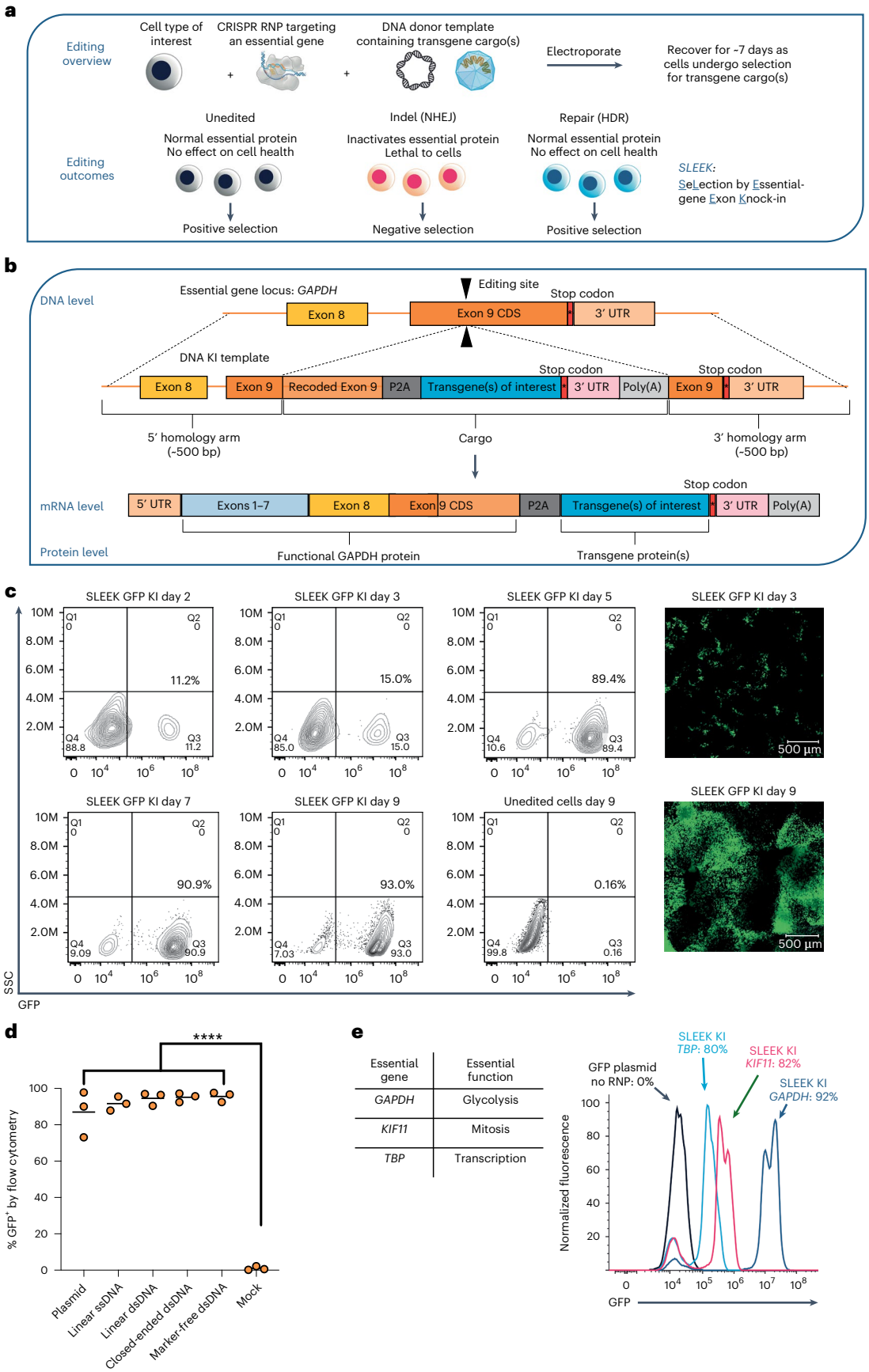

We asked whether we could leverage other DNA templates that lacked unnecessary bacterial expression components. Both capabilities are very attractive for clinical manufacturing. We tested several DNA templates beyond circular double-stranded DNA (dsDNA) plasmid that lacked extraneous DNA sequences and genes that are part of normal plasmid backbones. This included linear single-stranded DNA (ssDNA), linear dsDNA, closed-ended dsDNA and marker-free circular dsDNA and demonstrated SLEEK KI efficiencies of 90–95.6% for all DNA templates tested (Fig. 1d).

SLEEK can be used to insert up to four transgene cargos in a single cassette

We next tested whether we could integrate and express multiple cargos in a single cassette. We found that we could efficiently KI multiple cargos with a bicistronic GFP-mCherry cargo (Supplementary Fig. 3a), and colonies that grew out from single cells were positive for both cargos as indicated by fluorescence microscopy (Supplementary Fig. 3b). We demonstrated both efficient bicistronic KI using P2A, T2A or IRES linkers (Supplementary Fig. 3c,d) as well as bi-allelic KI of two different genes from two different plasmids, one containing GFP and the other containing mCherry (Supplementary Fig. 3e,f). We then showed that we could use SLEEK to efficiently insert a 5kb KI cassette with four gene cargos: CD16:mbIL-15:GFP:mCherry (Supplementary Fig. 4a). We validated expression of all detectable cargos in iPSCs by flow cytometry, showing each of them appearing in more than 90% of iPSCs other than CD16, which is not expressed in iPSCs as it requires adaptor proteins[11,12] that are present only in mature immune cells (Supplementary Fig. 4b–d). Of note, the mean fluorescence intensity (MFI) of the GFP cargo in the third position in the four-cargo cassette was 37.5-fold lower than when GFP was the only cargo in the cassette (Supplementary Fig. 4e), indicating that important consideration is needed in selecting cargo position in a multi-cistronic SLEEK KI cassette, with cargos requiring higher expression positioned at the front (5′ end) and cargos where lower expression is desired positioned at the back (3′ end).

Expression of transgene cargo is tunable by SLEEK KI at different essential genes

Beyond controlling gene expression by selecting the position order of cargos in a multi-KI cassette, we reasoned that cargo expression could also be tuned through SLEEK KI at other essential genes. There is strong interest in being able to carefully control cargo expression for different iPSC-derived cell therapy applications[17]. We reasoned that, by performing SLEEK at other essential genes, we could harness the intrinsic promoter strengths of those endogenous genes to achieve our desired cargo expression as well as providing optionality for the introduction of different transgenes at multiple SLEEK sites in parallel. We show this in practice at two other essential genes: *TBP* (TATA-binding protein) and *KIF11* (kinesin family member 11)[26,27]. The MFI of the GFP cargo at these sites varied from each other and from *GAPDH* by 10-fold to 100-fold, demonstrating broad tunability of transgene cargo expression levels with SLEEK (Fig. 1e).

SLEEK works across clinically relevant cell types and with different DNA formats

We then asked if SLEEK could be used across other primary cell types beyond iPSCs. We tested SLEEK KI of GFP cargos using AAV6 DNA templates in primary B cells, NK cells and T cells (Fig. 2a). SLEEK KI rates are shown for all cell types (Fig. 2b,c) and are higher than the best previously reported KI efficiencies achieved in B cells[28], NK cells[19,29] and T cells[19]. We then compared the efficiency and potency of SLEEK-based KI at the *GAPDH* locus to the current standard T cell receptor α constant (*TRAC)* locus KI strategy with an AAV6 DNA template in T cells[17,19] and also with an HDR enhancer small molecule[30] to maximize the *TRAC* KI efficiency (Fig. 2d). SLEEK KI is more than 100-fold more potent than the standard AAV6 KI at the *TRAC* locus (Fig. 2d), demonstrating that SLEEK not only achieves greater KI efficiency overall but also can do so using substantially lower concentrations of AAV6 KI template (Supplementary Fig. 5a). Maximal KI efficiencies for both methods were tested both with and without an HDR enhancer and showed only slight improvement; this indicates that HDR enhancer may be dispensable with SLEEK (Fig. 2e). We then assessed T cell viability and expansion for the SLEEK KI strategy compared to the standard *TRAC* KI strategy over 7 days and showed that both viability (Fig. 2f) and expansion (Fig. 2g and Supplementary Fig. 3b,c) are similar to *TRAC* KI T cells. We went further in assessing SLEEK KI T cell expansion and showed no detrimental impact on total T cell number after 19 days in culture compared to *TRAC* KI (Supplementary Fig. 5b). Finally, we tested if SpCas9 could be used to achieve SLEEK KI in T cells when targeting the same *GAPDH* SLEEK site with the same AAV6 GFP template used with AsCas12a (Supplementary Fig. 5c). SLEEK KI of GFP cargo using an SpCas9 RNP was assessed by flow cytometry after 7 days and shown to be 92.0% efficient, similar to the efficiency observed with AsCas12a (Supplementary Fig. 5d,e). Therefore, SLEEK KI in T cells is readily amenable to other nucleases, assuming they can edit the target site in an essential gene with high efficiency.

Owing to well-documented manufacturing challenges associated with AAV and other viral vectors[20], we asked whether SLEEK could enable efficient KI using non-viral DNA templates in T cells. Non-viral DNA templates have previously been shown to be more toxic and less efficient at KI than AAV6, thus limiting their potential[31–33], although recent progress has led to efficiencies of more than 50% in T cells[34]. We leveraged and optimized a recently described T cell protocol (Methods) for linear dsDNA and ssDNA templates (Fig. 2h). When comparing SLEEK GFP KI efficiencies (Fig. 2i), day 7 viability (Fig. 2j) and fold expansion (Fig. 2k) with these different DNA templates, we saw minimal differences between ssDNA templates and AAV6. Linear dsDNA, however, showed slightly lower viability and expansion on day 7 compared to ssDNA, AAV6 and mock-treated T cells, which is consistent with other studies[31]. We further examined the use of next-generation circular dsDNA templates, which do not contain the kanamycin resistance marker or other conventional bacterial expression plasmid elements, as well as closed-ended linear DNA templates (Supplementary Fig. 6a) and demonstrated efficiencies of more than 91.7% for all DNA template types other than circular dsDNA (Supplementary Fig. 6b). Moreover, we show that there is no absolute requirement for an HDR enhancer to achieve high SLEEK KI rates in human primary T cells (Supplementary Fig. 6c) with non-viral DNA templates.

Editing with the SLEEK RNP is highly specific with no verified off-targets

With SLEEK able to achieve nearly 100% transgene KI with both viral and non-viral templates, we postulated that this technology could be of great potential value for generating cell therapies. To support this assertion, it is critical to characterize off-target activity of the SLEEK approach at the *GAPDH* site. We identified candidate off-target sites through a combination of orthogonal specificity assays, including in silico (CALITAS)[35], cellular (GUIDE-Seq)[36] and biochemical (Digenome-Seq)[37] (Supplementary Fig. 7a). Candidate off-target sites from each of the three specificity assays were then assessed in T cells using a multiplex PCR-NGS rhAmpSeq method[24] to determine whether any off-target candidates could be verified. We found that no candidate off-target sites were verified by rhAmpSeq with a sensitivity of 0.1%, demonstrating that the SLEEK RNP is highly specific (Supplementary Fig. 7b).

On-target sequencing data shows high transgene insertion across DNA templates

Beyond analysis of small indels at on-target and off-target sites, the gene editing field has continued to uncover other potentially undesirable editing outcomes, such as large resections[38], translocations between on-target edited alleles[39] and improper KI of the donor HDR construct[40].

https://doi.org/10.1038/s41587-023-01779-8

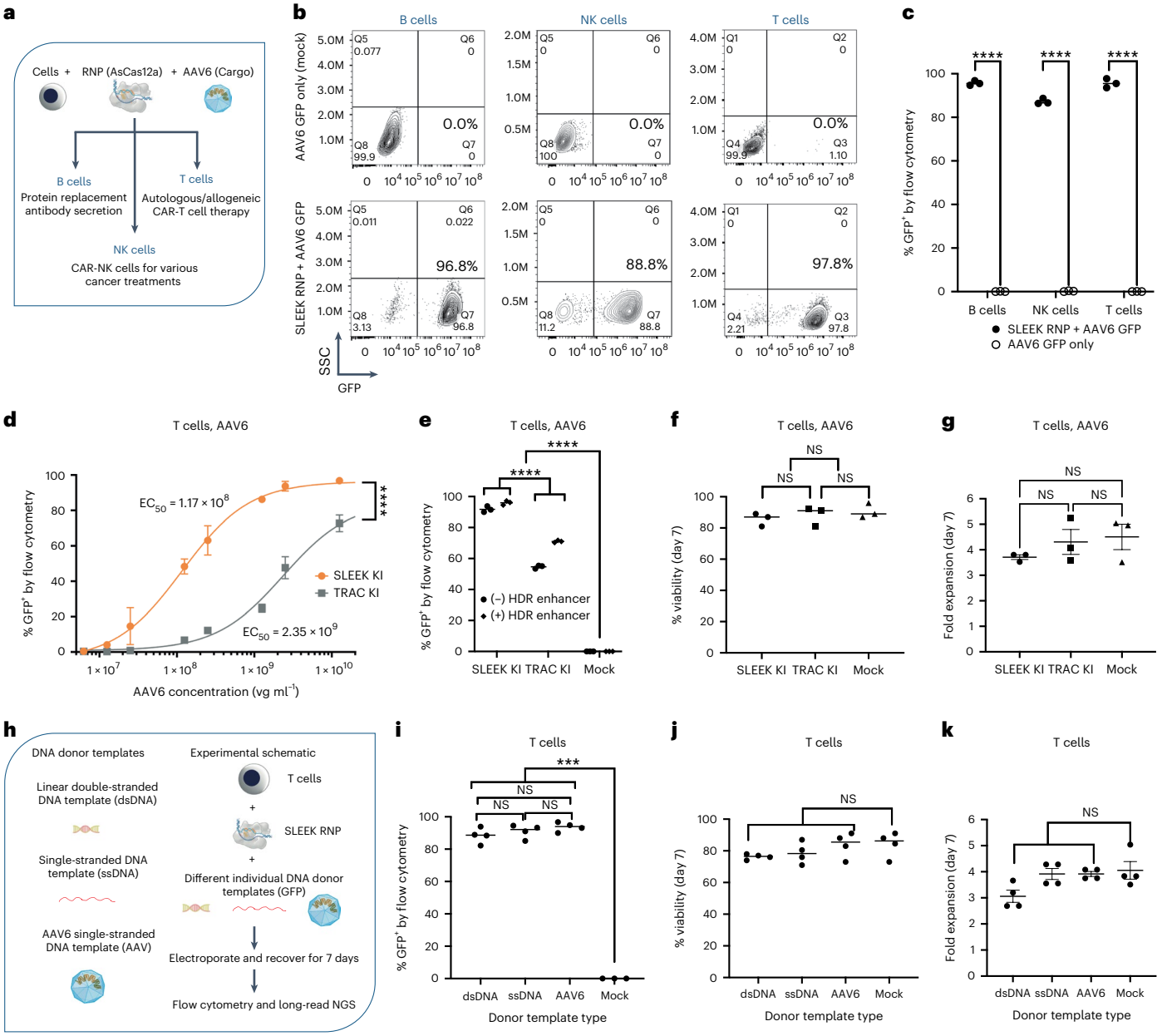

Fig. 2 | SLEEK generates superior KI efficiencies to current strategies across cell types. a, Demonstration of possible applications for SLEEK KI using AAV6 current standard in different clinically relevant cell types. **b**, SLEEK KI of GFP cargos into primary B cells, primary NK cells and primary T cells with AAV6 DNA template as measured by flow cytometry after 7 days. **c**, Plotting of SLEEK KI efficiencies for these three cell types as measured by GFP$^+$ cells by flow cytometry. $n = 3$ independent experiments; black lines indicate means; two-way ANOVA, Sidak's multiple comparisons test, $^{****}P < 0.0001$. **d**, Comparison of GFP KI efficiency and potency in human primary T cells as a function of AAV6 viral concentration for SLEEK KI and *TRAC* KI strategies measured by flow cytometry after 7 days. HDR enhancer was added to both conditions to allow for maximal efficiency for the *TRAC* KI condition. $n = 3$ independent experiments; error bars represent mean ± s.d.; two-way ANOVA, Sidak's multiple comparisons test, $^{**}P < 0.01$, $^{****}P < 0.0001$. **e**, Day 7 measurement of SLEEK KI efficiency compared to *TRAC* KI strategy leveraging AAV6 cargo template with and without HDR enhancer, with both conditions leveraging engineered AsCas12a and cargo constructs that mainly differ only in homology arms surrounding the GFP cargo and the restored final portion of the *GAPDH* exon in the case of SLEEK. **f**, Viability of SLEEK KI compared to *TRAC* KI and mock-treated T cells after 7 days. **g**, Fold expansion of SLEEK-edited T cells compared to either *TRAC* locus KI T cells or mock-treated T cells after 7 days. **h**, Testing of non-viral DNA templates with SLEEK as a potential substitute for current AAV6-based KI strategies. SLEEK GFP KI efficiencies were measured in T cells using linear dsDNA or ssDNA templates and compared to an AAV6 DNA template, with all conditions assessed for GFP KI by flow cytometry after 7 days. **i**, SLEEK KI efficiencies of different non-viral and viral GFP cargo DNA templates compared to mock-treated cells as measured by flow cytometry after 7 days. SLEEK KI samples were compared to mock-treated T cells. **j**, Viability of SLEEK KI for different DNA templates compared to mock-treated T cells as measured by flow cytometry after 7 days. **k**, Fold expansion of SLEEK-edited T cells using different DNA templates compared to mock-treated T cells after 7 days. Data are presented as mean ± s.e.m. (**g**,**k**) of ≥3 biological replicates and analyzed by one-way ANOVA (**e**–**g** and **I**–**k**) followed by Bonferroni's multiple comparisons test or two-way ANOVA (**c**) followed by Sidak's multiple comparisons test. Data points indicate replicates; lines indicate means. Pairwise comparisons are not statistically different unless otherwise indicated by $^{****}P < 0.0001$, $^{***}P < 0.001$, $^{**}P < 0.01$, $^{*}P < 0.05$. EC_{50}, half maximal effective concentration; NS, non-significant; SC, side scatter.

These editing outcomes can be assessed with Oxford Nanopore Technologies (ONT) long-read sequencing[41] and ddPCR. ONT long-read sequencing was employed to assess whether cargos were inserted fully intact, including 3′ distal to the *GADPH* SLEEK RNP cut site, and to assess the frequency of multiple cargo insertion events (Supplementary Fig. 8a–c). In some instances, multiple tandem insertions of the KI template were observed. This event occurs ~20% more with linear dsDNA templates than for linear ssDNA and AAV6 templates (Supplementary Fig. 8c). Based on GFP cargo expression in more than 90% of T cells by flow cytometry, and long-read sequencing data showing that the first SLEEK KI cargo contains an intact stop codon, 3′ untranslated region (UTR) and poly(A) binding sequence in most cases, it is evident that most multiple insertion events still result in expression of the SLEEK KI transgene of interest. Analysis of large resections using ONT long-read sequencing showed that detected deletions were smaller than ~800 base pairs (bp) (Supplementary Fig. 8e) and were only a small portion of the total number of reads detected. Of potential concern around *GAPDH*, we were specifically interested in the *CHD4* (chromodomain helicase DNA-binding protein 4) gene that resides approximately 30 kb away from the SLEEK RNP cut site, as it is the nearest gene relative to the SLEEK GAPDH site listed in the Cosmic Cancer Gene Census[42]. We used ddPCR to measure potential *CHD4* allelic dropout over multiple days. This was done both to assess whether these large resections occur and to determine whether these events become enriched over time. No allelic dropout of the *CHD4* gene was observed by ddPCR over 14 days (Supplementary Fig. 8f), which is consistent with the overall absence of resections of that size regardless of DNA template format used with SLEEK. Because the SLEEK RNP used has no detectable off-target editing, we did not generate data for possible random integrations of the transgene cassette. Random integrations, if present, are expected to be low for the different DNA templates used in this study. Overall, undesired editing outcomes for different DNA templates using SLEEK are low and consistent with what has been observed previously in the literature[38], with relatively few large resections (Supplementary Fig. 8e) and random integration of DNA template backbone components accounting for less than 10% of KI events across DNA template types (Supplementary Fig. 8b).

SLEEK can generate multiplex-edited allogeneic T cells with near homogeneity

Having shown that SLEEK works with reporter genes in multiple cell types and has a clinically attractive safety profile, we asked whether clinically relevant functional cargos can be inserted with SLEEK in established model systems to improve cellular activity against tumor cells. As a model for an autologous CAR-T drug product (Fig. 3a), we demonstrated SLEEK KI of a CD19 CAR at 95.8% efficiency (Fig. 3b and Supplementary Fig. 9a) and similar efficiency with other functional cargos compared to controls (Supplementary Fig. 9b). CD19 CAR SLEEK KI T cells led to robust cytolysis of tumor cells in vitro compared to controls (Fig. 3c). In addition, certain edits such as knockout (KO) of *TGFBR2* (transforming growth factor beta receptor 2) are considered promising for countering the presence of immune-suppressive TGF-β cytokine in the tumor microenvironment[43], supporting the need for additional edits in combination with SLEEK KI of a CD19 CAR (Supplementary Fig. 9c). We confirmed that *TRAC* KO and *TGFBR2* KO edits were highly efficient by NGS when paired with SLEEK KI of either CD19 CAR or GFP cargos (Supplementary Fig. 9d). We then combined *TGFBR2* KO with SLEEK KI of a CD19 CAR and showed robust cytolysis of tumor cells in vitro compared to controls (Supplementary Fig. 9e,f). We next modeled a case requiring multiplexed editing with SLEEK. We show the sets of edits likely needed to generate an allogeneic T cell (Fig. 3d), which likely requires KO of the endogenous T cell receptor (TCR) through KO of the *TRAC* gene, KO of major histocompatibility complex-I (MHC-I) through KO of the *B2M* (beta-2-microglobulin) gene and KO of major histocompatibility complex-II (MHC-II) through KO of the *CIITA* (major histocompatibility class II transactivator) gene. These edits would be paired with SLEEK KI of either a CD19-CAR alone or a bicistronic CD19 CAR in tandem with a B2M–HLA-E fusion construct, commonly referred to as an NK Shield[44] (Supplementary Fig. 10a). These allogeneic T cell edits are designed to protect the host from a graft versus host response from the SLEEK KI engineered T cell while also protecting the SLEEK KI engineered T cells from $CD4^+$ (MHC-II) and $CD8^+$ (MHC-I) host versus graft T cell responses. In addition, SLEEK KI of an NK Shield should protect the SLEEK KI T cells from host NK cells, despite them being MHC-I negative (*B2M* KO) and otherwise expected to be susceptible to NK cell-mediated lysis. The B2M–HLA-E NK Shield construct will interact with a well-known NK cell inhibitory receptor, NKG2A. Through this interaction, NK cell effector function is suppressed, leading to a protective benefit for SLEEK KI cells. To first test the SLEEK CAR KI alone, we observed that 98.6% of cells were negative for TCR and MHC-I, and 86.1% of all cells expressed the CD19 CAR by flow cytometry (Fig. 3e and Supplementary Fig. 10b). Treatment of NALM6 tumor cells with triple-KO T cells also containing SLEEK KI of a CD19 CAR led to robust cytolysis (Fig. 3f). For the bicistronic SLEEK KI experiment, we confirmed *TRAC*, *B2M* and *CIITA* editing by NGS (Supplementary Fig. 10c). These multiplex-edited allogeneic T cells were then assessed for KI of

Fig. 3 | SLEEK enables multiplex editing and near-homogeneous KI of functional cargos in primary T cells and NK cells. a, Schematic of how SLEEK could be used to KI a CAR or engineered T cell receptor (eTCR) for applications such as autoimmunity or oncology. **b**, Demonstration of SLEEK KI efficiency with different cargos after 7 days. Data are plotted with mean from three biological replicates, with differences determined to be non-significant, as measured by one-way ANOVA followed by Bonferroni's multiple comparisons test. **c**, Testing of either a SLEEK KI CD19 CAR or a SLEEK KI GFP control in T cells against Raji tumor cells. Cytotoxicity was assessed using an LDH release assay after 24 h of co-culture at an E:T ratio of 2:1 with T cells that received SLEEK KI 7 days prior. Average spontaneous LDH release by Raji cells and LDH released upon treatment with lysis buffer are provided for comparison. Filled circles indicate data from four technical replicates from each of one biological sample; black lines indicate means; $^{****}P < 0.0001$. **d**, Schematic of how SLEEK could be used in conjunction with multiplex editing to generate allogeneic T cells with potential immune evasion. **e**, Assessment of SLEEK multiplex KO and KI efficiency in T cells by a combination of flow cytometry and NGS with flow cytometry used to confirm both phenotypic TCR (*TRAC*) and MHC-I (*B2M*) KO cells that also contain either a CD19 CAR or GFP KI. KO of MHC-II (*CIITA*) was measured by NGS; KO of TCR (*TRAC*) and MHC-I (*B2M*) was measured by both methods. The % total events captures all cells containing the noted edit within the bulk population by either flow cytometry and/or NGS after 7 days. $^{****}P < 0.0001$. **f**, Testing of allogeneic T cell KO edits paired with SLEEK CD19 CAR KI or GFP KI, as well as SLEEK CD19 CAR KI only, against NALM6 tumor cells and unedited T cells 7 days after editing. Cytotoxicity was assessed using an LDH release assay after 24 h of co-culture at an E:T ratio of 1:1. Average spontaneous LDH release by NALM6 cells and LDH released upon treatment with lysis buffer are provided for comparison. Filled circles indicate data from four technical replicates from each of one biological sample; black lines indicate means. No other pairwise comparisons of CD19 CAR edit configurations reveal statistically significant differences in mean. **g**, Schematic of how SLEEK could be used to generate an allogeneic engineered NK cell medicine. **h**, Demonstration of SLEEK KI of a CD19 CAR or GFP control cargo as measured by flow cytometry 7 days after editing. Both cargo KI efficiencies are plotted with mean from three biological replicates, with differences in efficiency determined to be non-significant, as measured by two-tailed unpaired *t*-test. **i**, Testing of either a SLEEK KI CD19 CAR or a SLEEK KI GFP control in NK cells against NALM6 tumor cells. Cytotoxicity was assessed using a DELFIA TRF cytotoxicity assay after 2 hours of co-culture at an E:T ratio of 1:1 on NK cells 7 days after editing. Average BATDA ligand released by NALM6 cells and BATDA ligand released upon treatment with lysis buffer are provided for comparison. Filled circles indicate data from eight technical replicates from each of one biological sample; black lines indicate means; $^{****}P < 0.0001$. NS, non-significant. Data are presented as mean ± s.e.m. and analyzed by two-tailed unpaired *t*-test (**b**,**h**,**i**) or one-way ANOVA (**c**,**e**,**f**) followed by Bonferroni's multiple comparisons test.

https://doi.org/10.1038/s41587-023-01779-8

both cargos, and we observed that 96.2% of T cells were negative for HLA-A/B/C, confirming KO at *B2M*, and 91% positive for both the CD19 CAR and the NK Shield (Supplementary Fig. 10d,e). We next validated the functionality of the NK Shield[44] cargo to protect MHC-I$^-$ T cells (*B2M* KO) from lysis by NK cells (Supplementary Fig. 11a–c). We showed that the NK Shield reduced NK lysis as measured by a CD107a degranulation assay (Supplementary Fig. 11d–g). Having validated that the allogeneic T cell edits could be made with high efficiency and paired with SLEEK KI of a CAR and NK Shield using the preferred AAV6 template, we wanted to show if we could achieve these types of SLEEK KI edits with non-viral templates. We showed SLEEK KI of these clinically important cargos, demonstrating SLEEK KI of a CD19 CAR (Supplementary Fig. 12a) at 82.4% efficiency and separately showed SLEEK KI of an EGFR CAR (Supplementary Fig. 12b) at 86.6% efficiency by flow cytometry. We next demonstrated SLEEK KI of the CD19 CAR and NK Shield bicistronic cargo at 70.0% efficiency with a linear dsDNA template (Supplementary Fig. 13c–e). Taken together, we demonstrate that SLEEK can be used for multiplex editing to generate clinically important allogeneic T cell products that can target and kill tumor cells while also being protected from a host versus graft response.

Minimal genotoxicity concerns for generating allogeneic T cells with SLEEK

With any multiplex editing application, it is necessary to assess translocation frequencies and possible enrichment of cells with undesirable outcomes during multiplex editing in primary human T cells.

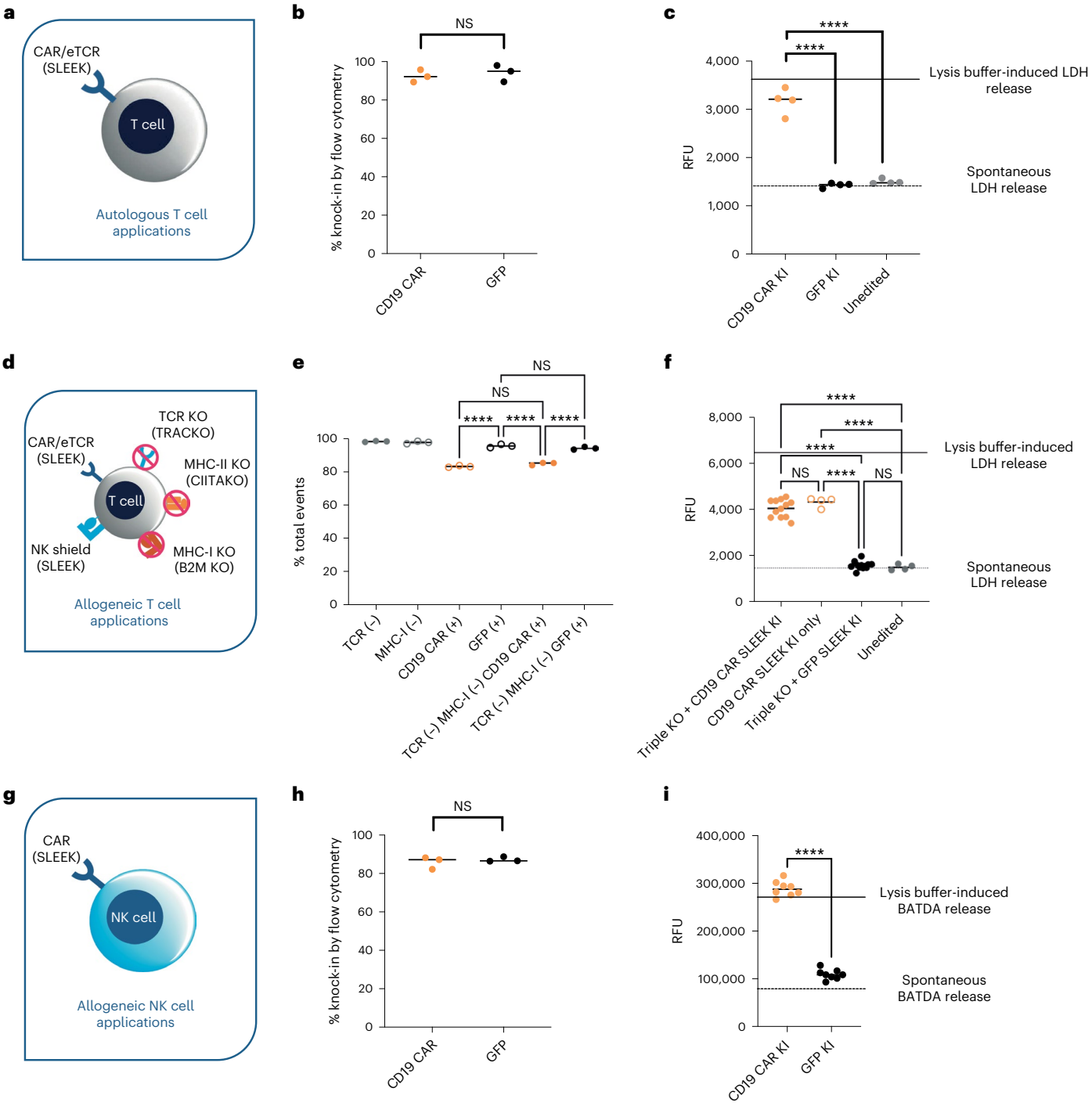

https://doi.org/10.1038/s41587-023-01779-8

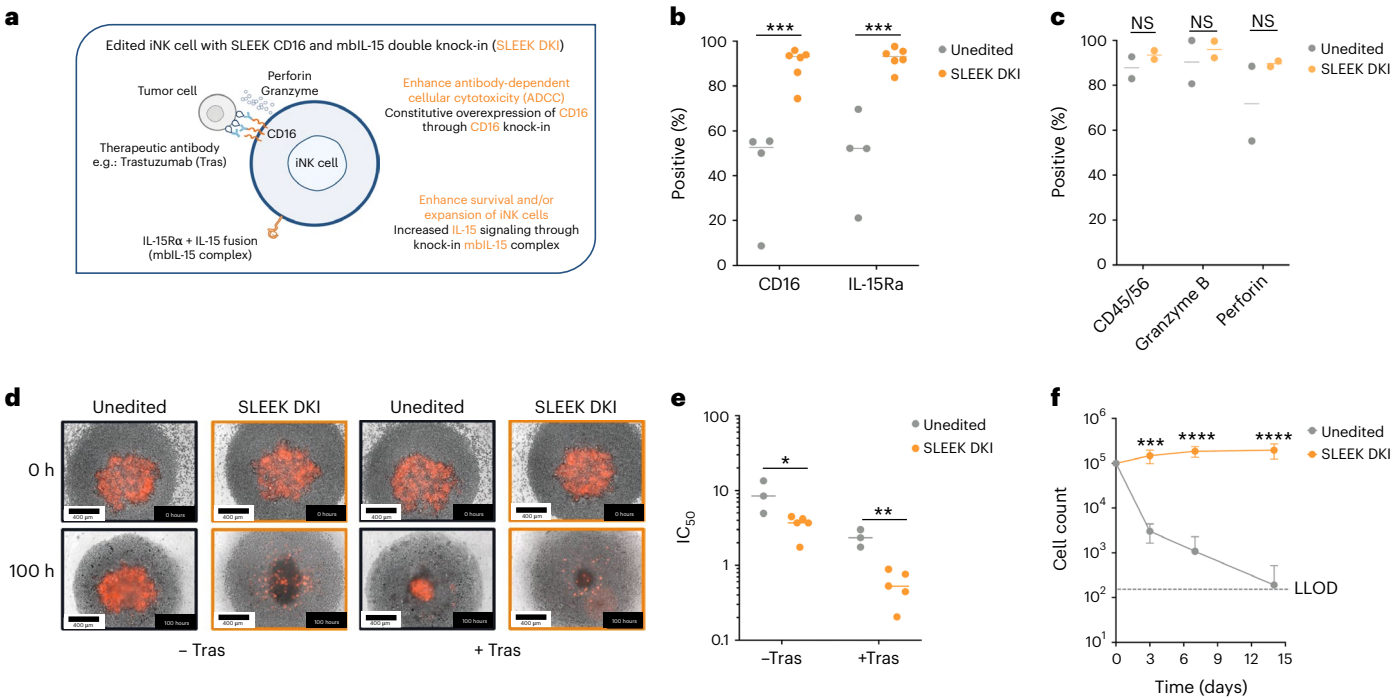

Fig. 4 | SLEEK DKI of CD16 and mbIL-15 into iPSCs led to efficient ADCC killing of tumor cells and increased persistence with differentiated iNK cells. **a**, Expression of CD16 and mbIL-15 cargos are proposed to be critical for ADCC and persistence, respectively. **b**, Flow cytometry was performed to determine the percentage of unedited or SLEEK DKI iNK cells that expressed each cargo. Each dot represents a single measurement of a unique differentiated iNK population derived from a unique iPSC clone, with lines representing medians. $n = 4–6$; four independent experiments with three SLEEK clones. **c**, Unedited and SLEEK DKI iNK cells were assessed by flow cytometry to confirm $CD45^+/CD56^+$ ratio and for expression of intracellular cytolytic granules perforin and granzyme B, with lines representing medians. $n = 2$ independent experiments. **d**, A 3D tumor spheroid assay with SKOV-3 cells was established using an E:T ratio of 10:1 along with inclusion or exclusion of trastuzumab. **e**, iNK cells were added at various E:T ratios, starting at 31.6:1 and ending with 0.01:1, with inclusion or exclusion of trastuzumab, IL-15 and TGF-β, and quantitative representation of two independent experiments with IC_{50} values is shown. $n = 3–5$; two independent experiments performed in singlet or doublet technical repeats with three SLEEK DKI clones. **f**, Unedited and SLEEK DKI iNK cells were cultured in basal media without supporting cytokines for 14 days. Data are presented as mean ± s.e.m. of two independent experiments performed in singlet or doublet technical replicates and analyzed by two-way ANOVA (**b**,**c**,**e**,**f**) followed by Sidak's multiple comparisons test. Data points represent technical duplicates, with lines representing the median. Pairwise comparisons are not statistically different unless otherwise indicated. $^*P < 0.05$, $^{**}P < 0.01$, $^{***}P < 0.001$, $^{****}P < 0.0001$. IC_{50}, half maximal inhibitory concentration; LLOD, lower limit of detection for assay; NS, non-significant; Tras, trastuzumab.

We summarize the types of expected translocation types that could arise during a multiplex editing experiment, in this case noting those that include TRAC and B2M RNPs for making an allogeneic T cell and the GAPDH SLEEK RNP for transgene KI of functional cargos (Supplementary Fig. 13a). Because all RNPs had no verified off-targets, with both AsCas12a TRAC and B2M RNP specificities reported previously[45] and the AsCas12a GADPH SLEEK RNP specificity analysis presented in this study (Supplementary Fig. 7a), translocation assays were built around all possible on-target to on-target translocation events (Supplementary Fig. 7a). All translocation types (acentric, dicentric and balanced) were measured by ddPCR on days 3, 5 and 7 after editing in combination with SLEEK KI (Supplementary Fig. 13b). The total set of possible translocations was then stacked and plotted, showing a notable reduction in total translocations across type from day 3 to day 7 (Supplementary Fig. 13c) with the drop off of acentric, dicentic and balanced translocations to less than 0.4% by day 7 (Supplementary Fig. 13d), similar to previous reports that also involved *TRAC* and *B2M* multiplex editing[39]. We note that one advantage of the SLEEK edit at *GAPDH* is that translocations to this essential gene should generally disrupt GAPDH protein function and be deleterious, suggested by their overall absence by day 7. Lastly, the presence of multiple DSBs has been shown to lead to elevated phosphorylation of H2A histone family member X (H2AX)[46] or enrichment of cells with either null or elevated tumor protein 53 (p53) phosphorylation[47]. To address this potential concern, we measured possible changes in post-translational modifications of these two key DNA damage markers in unedited and SLEEK KI T cells measured at 7 days and 14 days after editing (Supplementary Fig. 13e). We did observe a modest increase in H2AX protein phosphorylation by a phospho-H2AX ELISA assay, indicating small increases in H2AX phosphorylation, which would be expected after multiplex editing (Supplementary Fig. 13f). However, we did not observe any changes in p53 phosphorylation by a phospho-p53 ELISA assay, indicating that multiplex editing paired with SLEEK KI did not lead to an enrichment in the cell population for T cells with null p53 function (Supplementary Fig. 13g). Overall, these data support the notion that using SLEEK at the *GAPDH* locus has limited genotoxicity concerns and would be safe when incorporated into an edited cell medicine.

SLEEK KI of CD19 CAR led to enhanced tumor killing in healthy donor NK cells

Finally, we tested whether human healthy donor NK (HDNK) cells could be engineered with functional cargos, such as a CAR, using SLEEK (Fig. 3g). NK cell medicines have, to date, shown a more attractive safety profile than T cell medicines in the clinic but are harder to manipulate through gene editing, in part due to their slower cycling times, which would impact levels of key HDR machinery proteins, and have shown higher sensitivity to foreign DNA[7]. Combining our own optimization efforts with those highlighted in a recent report[7], we were able to achieve 86.6% CD19 CAR SLEEK KI and 87.2% GFP SLEEK KI in human HDNK cells using an AAV6 template (Fig. 3h and Supplementary

Fig. 14a–c). These CD19 CAR-NK cells achieved greater tumor cytolysis compared to GFP SLEEK KI control NK cells on NALM6 tumor cells (Fig. 3i). Taken together, we show that SLEEK KI of functional cargos led to efficient KI and subsequent beneficial functional outcomes in vitro in both T cells and NK cells, suggesting that SLEEK can enable the generation of near-homogeneous editing in T cell and NK cell medicines.

SLEEK double knock-in of CD16 and mbIL-15 led to potent iNK-mediated tumor killing in vitro

To generate a highly functional iPSC-derived NK cell for addressing solid tumors, we first determined whether SLEEK technology could be used to achieve bicistronic KI of CD16 and mbIL-15 into iPSCs and whether this would lead to efficient ADCC killing of tumor cells upon differentiation into iNK cells (Fig. 4a and Supplementary Fig. 15a). We designed a bicistronic construct with both CD16 and mbIL-15, separated by a P2A sequence. First, we sought to determine if SLEEK KI at *GAPDH* would affect GAPDH protein levels, cell metabolism and growth rate during the 39-day differentiation process for generating iNK cells. The presence of GAPDH protein (Supplementary Fig. 15b) was verified by western blot as well as the CD16 protein, which directly followed the P2A. Lower levels of both the GAPDH protein and the CD16 protein cargo (Supplementary Fig. 15c) were observed in iPSCs heterozygous for the SLEEK KI cassette compared to the iPSCs homozygous for the SLEEK KI cassette, as would be expected. Observing this, we moved forward with a homozygous bicistronic SLEEK double knock-in (DKI) clone. For the SLEEK homozygous KI clone, we assessed GAPDH mRNA transcript levels by reverse transcriptase quantitative PCR (RT–qPCR) and observed 42.37% lower GAPDH mRNA levels in multiple SLEEK KI clones compared to unedited iPSC clones (Supplementary Fig. 15d). This difference was not unexpected given that we have replaced the endogenous GAPDH mRNA 3′ UTR with the SLEEK KI cassette exogenous 3′ UTR. To determine if this lower mRNA level at the iPSC stage had any notable impact on cell proliferation, we plated clones and assessed growth rates for SLEEK DKI and unedited iPSCs over 5 days, and no difference in growth rates was observed (Supplementary Fig. 15e). This lack of effect on cell metabolism was further supported by lack of any difference in viability (Supplementary Fig. 15f) or glucose consumption (Supplementary Fig. 15g) between unedited and SLEEK DKI iPSCs after 5 days. Analysis of metabolic marker expression after 5 days by flow cytometry showed no difference between unedited and SLEEK DKI iPSCs (Supplementary Fig. 15h). We next sought to determine whether SLEEK DKI of CD16 and mbIL-15 led to differences in iPSC morphology, metabolic marker expression, pluripotency, cell growth and phenotype. Pluripotency was assessed by staining for iPSC pluripotency markers (OCT4, NANOG, SOX2 and TRA1-60). There was no appreciable difference between SLEEK DKI and unedited iPSCs, indicating that SLEEK DKI did not alter pluripotency (Supplementary Fig. 15i). Micrograph images of SLEEK DKI and unedited iPSCs showed densely packed cell colonies with well-defined borders after 1 week of culture, further supporting the notion that SLEEK does not alter iPSC stemness or morphology (Supplementary Fig. 15j). SLEEK DKI and unedited iPSCs were then differentiated into iNK cells and monitored for possible changes in metabolic marker expression, phenotype, cell growth and function. Both unedited and SLEEK DKI iNK cells proliferated at similar rates throughout the differentiation process (Supplementary Fig. 16a). At the end of differentiation, metabolic marker expression was measured by flow cytometry, and no difference between unedited and SLEEK DKI iNK cells was observed (Supplementary Fig. 16b). We measured iNK cell maturation and phenotype by flow cytometry, and, other than CD16, which is constitutively expressed as part of the SLEEK DKI cassette, all other NK cell markers were similar between SLEEK DKI and unedited iNK cells (Supplementary Fig. 16c). Notably, SLEEK DKI iNK cells showed similar GAPDH mRNA levels by RT–qPCR to unedited iNK cells as well as to peripheral blood NK cells isolated from healthy human donors. We attributed the discrepancy seen in the iPSC stage (Supplementary Fig. 15d) to the now robust expression of mbIL-15 driven off of the strong *GADPH* promoter in mature iNK cells, where IL-15 stimulation is known to stimulate NK cell metabolism[48] (Supplementary Fig. 16d). Upon stimulation with ionomycin, both SLEEK DKI and unedited iNK cells were able to produce interferon gamma (IFN-γ), indicative of successful differentiation to NK cells (Supplementary Fig. 16e). SLEEK DKI iNK cells showed 2-fold higher rates of CD16 and mbIL-15 surface expression of both KI cargos compared to unedited iNK cells (Fig. 4b and Supplementary Fig. 17a,b) while showing similar levels of CD45/56, perforin and granzyme B (Fig. 4c), indicating that we achieved highly functional NK cells from iPSCs at the end of the differentiation process. These results show that SLEEK KI has no negative effect on cell growth, cell metabolism or cell morphology or on the ability to be differentiated into an iNK cell.

We assessed cytotoxicity with a three-dimensional (3D) tumor spheroid assay on SKOV-3 cells, which are an ovarian cancer cell line positive for HER2. An effector-to-target (E:T) ratio of 10:1 was used to allow for clear resolution between natural cytotoxicity and ADCC. Conditions with or without 10 μg ml^{-1} of trastuzumab were used, and there was a marked reduction in live tumor cells in both conditions when compared to unedited iNK cells (Supplementary Fig. 17c,d). iNK cells were added at various E:T ratios, with or without trastuzumab, in the 3D tumor spheroid assay (Fig. 4d). SLEEK DKI iNK cells showed a 4.42-fold greater potency (IC_{50}) over unedited iNK cells in the presence of trastuzumab (Fig. 4e) and outperformed peripheral blood NK cells from healthy donor (Supplementary Fig. 17e). To assess whether SLEEK KI of mbIL-15 provided functional benefit, unedited and SLEEK DKI iNK cells were cultured in basal media without supporting cytokines for 21 days to assess persistence. Unedited iNK cell numbers were reduced 2–3 orders of magnitude by day 10, whereas SLEEK DKI iNK cells showed persistence over the course of the assay (Fig. 4f). Taken together, these results show that SLEEK is a powerful technology to drive high-level constitutive CD16 and mbIL-15 expression on the surface of iNK cells. The high-level constitutive CD16 expression enhanced ADCC and improved tumor killing, whereas the high-level mbIL-15 expression substantially increased the persistence of the SLEEK DKI iNK cells.

SLEEK DKI of CD16 and mbIL-15 led to potent iNK-mediated tumor killing in vivo

Having shown that SLEEK KI of CD16 and mbIL-15 led to potent tumor killing in vitro, we then evaluated the anti-tumor activity of SLEEK DKI iNK cells in a more clinically relevant mouse xenograft SKOV-3 ovarian tumor model. Mice were inoculated intraperitoneally (IP) with luciferase-expressing human SKOV3 cells and, 4 days later, received a single dose of 2.5 mg kg^{-1} of trastuzumab in combination with 5×10^6 unedited or SLEEK DKI iNK cells (Fig. 5a). No exogenous cytokines were administered for NK cell survival because we hypothesized that the high expression of mbIL-15 on SLEEK DKI iNK cells would be sufficient to support in vivo persistence. Before in vivo dosing, SLEEK DKI iNK cells were confirmed to have a higher frequency of $CD56^+CD16^+$ cells compared to unedited iNK cells, 100% and 53.3%, respectively (Supplementary Fig. 18a). Tumor burden was monitored by bioluminescent imaging (BLI) using an In Vivo Imaging System (IVIS) for 108 days (Fig. 5b). When compared to trastuzumab treatment alone or in combination with unedited iNK cells, SLEEK DKI iNK treatment with trastuzumab induced significant reduction in tumor burden, with the maximal response seen as early as day 11 after treatment (Supplementary Fig. 18b) and continued tumor control until day 54 (Supplementary Fig. 18c). The improved anti-tumor activity of SLEEK DKI iNK cells was compared to the isotype control, trastuzumab alone or unedited iNK cells with trastuzumab and resulted in undetectable tumor cells in four of eight mice during the study (Fig. 5c). Notably, treatment with SLEEK DKI iNK cells substantially improved survival compared to trastuzumab treatment alone or with unedited iNK cells, with all mice surviving in the SLEEK DKI group after 144 days in the study compared to 37.5% of

https://doi.org/10.1038/s41587-023-01779-8

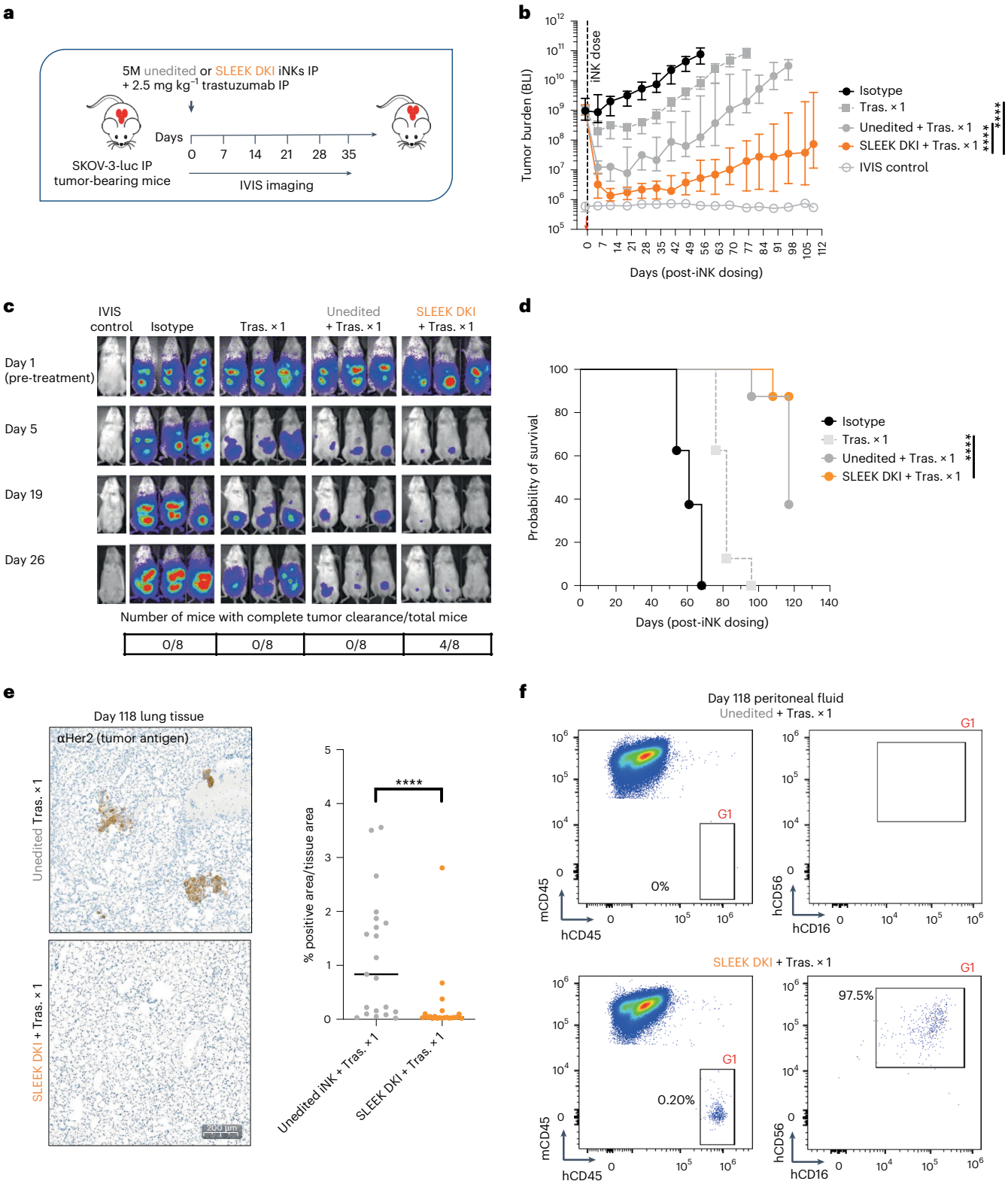

Fig. 5 | SLEEK DKI of CD16 and mbIL-15 led to potent iNK-mediated tumor killing in vivo. a, Schematic of experimental design for in vivo study using SKOV-3-luc IP tumor model. Black arrow represents IP iNK cell dosing, and red arrow indicates IP injection of trastuzumab. **b**, Tumor burden assessed by IVIS up to day 110 after iNK dosing, with the isotype positive control and IVIS negative control indicated on the plot. $n = 8$ mice per group. **c**, Bioluminescence images of representative timepoints showing tumor progression. **d**, Survival curves showing mice from previously described treatments. **e**, Histological analysis detecting human HER2 in the lung tissue showing reduced to no metastasis with SLEEK iNK treatment in combination with trastuzumab; scale, 200 µm. $n = 7$ wild-type mice and $n = 8$ iNK-treated mice. **h**, Ratios indicated are the number of mice with metastasis / total mice in treatment group. **f**, Representative flow cytometry plot gated on live mCD45$^-$hCD45$^+$hCD56$^+$hCD16$^+$ cells in mouse peritoneal fluid 118 days after NK cell treatment. $n = 2$ independent experiments. Data are presented as mean ± s.e.m. and analyzed by one-way ANOVA (**e**) followed by Bonferroni's multiple comparisons test or two-way ANOVA (**b**) followed by Bonferroni's multiple comparisons test or analyzed by Kaplan–Meier survival analysis (**d**) with log-rank (Mantel–Cox) test. *$P < 0.05$, **$P < 0.01$, ***$P < 0.001$, ****$P < 0.0001$. hCD16, human CD16; hCD45, human CD45; hCD56, human CD56; luc, luciferase; mCD45, mouse CD45; NS, non-significant; Tras, trastuzumab.

mice treated with unedited iNK cells and trastuzumab (Fig. 5d). At the conclusion of the study, we performed histological analysis by targeting Her2 in the lung tissue, which showed that treatment with SLEEK DKI iNK cells resulted in reduced metastasis compared to unedited iNK cells (Fig. 5e). We also investigated the in vivo persistence of both unedited and SLEEK DKI iNK cells by examining the blood (Supplementary Fig. 18d) and peritoneal fluid with flow cytometry. On day 118 after treatment, SLEEK DKI iNK cells were still present in the peritoneal fluid and expressed high levels of CD16 compared to unedited iNK cells (Fig. 5f), with unedited iNK cells being undetectable. The unprecedented in vivo persistence and high levels of CD16 were attributed to the high expression of mbIL-15 and CD16 driven off the strong *GAPDH* promoter. Taken together, we show that SLEEK DKI iNK cells administered as an IP injection in combination with a single dose of trastuzumab induced robust anti-tumor activity, resulting in reduced tumor burden and a statistically significant survival benefit, providing a potential therapeutic option for solid tumor cancers.

Discussion

SLEEK achieves higher KI levels in iPSCs, B cells, NK cells and T cells than current technologies, including those that leverage AAV6 DNA templates. This should lead to the generation of more homogenous cell medicines, improving both efficacy and safety in the clinic[9,49]. Furthermore, because SLEEK works with equivalent efficiency with either AAV6 or non-viral DNA templates, SLEEK should enable faster manufacturing of cell therapies, with lower potential costs and with fewer cargo size limitations. Although the current size limitations of ~5 kb for both ssDNA and AAV6 DNA templates may limit the number and types of cargo possible in such SLEEK KI cassettes in certain cases, because SLEEK does not rely on an exogenous promoter in the KI cassette, SLEEK can leverage larger cargo capacities than most other methods with these two attractive delivery modalities. Furthermore, the ability to use linear dsDNA templates at lower concentrations with SLEEK greatly reduces their intrinsic toxicity and should allow for much larger multi-cistronic cargos in T cells for both research and potential clinical applications. This should enable engineered cell medicines that successfully harness more sophisticated multi-cargo cassettes likely needed to address highly complex diseases, such as cancer. Although there are attractive reasons to leverage the endogenous *TRAC* locus for KO/KI to drive cargo expression off the physiologically relevant *TRAC* promoter in T cells[17], because SLEEK KI at *GAPDH* relies on an expression of an essential gene, it not only works well in T cell applications but also should be compatible with the vast majority of other cell types. Furthermore, tunability of cargo expression has been shown to be critical for optimal in vivo performance for CAR-T[50]. SLEEK enables fine-tuning of cargo expression by leveraging hundreds of available essential human genes, with each locus providing unique endogenous expression levels to provide optimal solutions for each unique research and clinical endeavor. Further characterization of these other candidate sites merits important future testing with this technology.

A key benefit of SLEEK KI at *GAPDH* is the ability to achieve stable and robust expression of multiple transgene cargos in the same cassette. A key example of this feature is the high and consistent level of CD16 cargo expression that we achieved, mitigating the need to use a non-cleavable CD16 construct[12,51] to maintain CD16 surface expression. This is an important result as previous studies have shown that if CD16 is not able to successfully detach from the target cell then this results in an increase in NK cell death[11]. The high-level constitutive CD16 expression enhances iNK ADCC and is expected to exert enhanced anti-tumor activity in the clinic. Additionally, we show that CD16/mbIL-15 SLEEK DKI iNK cells have unprecedented in vivo persistence without exogenous cytokine support, which could be an important safety advantage in the clinic. Conversely, in cases where lower expression levels are desired, placement in later positions in the cassette can allow expression to be lowered >10-fold as shown with the 5kb 4 cargo KI cassette. We have demonstrated multiple examples of tunability with SLEEK, namely both the choice of essential gene endogenous promoter and the position of the cargo in a multi-cistronic SLEEK KI cassette. Future iterations of the iNK modality or other iPSC-derived cell types could leverage this tunability, especially in cases where lower expression is advantageous, or even necessary, during the differentiation process.

This work demonstrates a technology to drive high-level transgene KI and expression of clinically relevant cargos across clinically relevant cell types. SLEEK has the potential to drive the next generation of cell-based medicines by achieving nearly complete homogeneity in populations of engineered cells containing many KO and KI edits, to enable broad tunability of expression for multi-transgene cargos and to accelerate the use of non-viral delivery formats to both democratize basic and translational research as well as accelerate clinical manufacturing. The last outcome may finally provide a tangible reduction in the cost of cell-based medicines, fulfilling the promise of this emerging class of medicines to reach broader patient populations.

Online content

Any methods, additional references, Nature Portfolio reporting summaries, source data, extended data, supplementary information, acknowledgements, peer review information; details of author contributions and competing interests; and statements of data and code availability are available at https://doi.org/10.1038/s41587-023-01779-8.

References

1. Bailey, S. R. & Maus, M. V. Gene editing for immune cell therapies. *Nat. Biotechnol.* **37**, 1425–1434 (2019).
2. Raffin, C., Vo, L. T. & Bluestone, J. A. Treg cell-based therapies: challenges and perspectives. *Nat. Rev. Immunol.* **20**, 158–172 (2020).
3. Wilkinson, A. C., Igarashi, K. J. & Nakauchi, H. Haematopoietic stem cell self-renewal in vivo and ex vivo. *Nat. Rev. Genet.* **21**, 541–554 (2020).
4. Raje, N. et al. Anti-BCMA CAR T-cell therapy bb2121 in relapsed or refractory multiple myeloma. *N. Engl. J. Med.* **380**, 1726–1737 (2019).
5. Abramson, J. S. Anti-CD19 CAR T-cell therapy for B-cell non-Hodgkin lymphoma. *Transfus. Med. Rev.* **34**, 29–33 (2020).
6. Frigault, M. J. et al. Tisagenlecleucel CAR T-cell therapy in secondary CNS lymphoma. *Blood* **134**, 860–866 (2019).
7. Naeimi Kararoudi, M. et al. Optimization and validation of CAR transduction into human primary NK cells using CRISPR and AAV. *Cell Rep. Methods* **2**, 100236 (2022).
8. Xie, G. et al. CAR-NK cells: a promising cellular immunotherapy for cancer. *EBioMedicine* **59**, 102975 (2020).
9. Liu, E. et al. Use of CAR-transduced natural killer cells in CD19-positive lymphoid tumors. *N. Engl. J. Med.* **382**, 545–553 (2020).
10. Depil, S., Duchateau, P., Grupp, S. A., Mufti, G. & Poirot, L. 'Off-the-shelf' allogeneic CAR T cells: development and challenges. *Nat. Rev. Drug. Discov.* **19**, 185–199 (2020).
11. Srpan, K. et al. Shedding of CD16 disassembles the NK cell immune synapse and boosts serial engagement of target cells. *J. Cell Biol.* **217**, 3267–3283 (2018).
12. Snyder, K. M. et al. Expression of a recombinant high affinity IgG Fc receptor by engineered NK cells as a docking platform for therapeutic mAbs to target cancer cells. *Front. Immunol.* **9**, 2873 (2018).
13. Hu, W., Wang, G., Huang, D., Sui, M. & Xu, Y. Cancer immunotherapy based on natural killer cells: current progress and new opportunities. *Front. Immunol.* **10**, 1205 (2019).
14. Szmania, S. et al. Ex vivo-expanded natural killer cells demonstrate robust proliferation in vivo in high-risk relapsed multiple myeloma patients. *J. Immunother.* **38**, 24–36 (2015).

15. Giron-Michel, J. et al. Membrane-bound and soluble IL-15/IL-15Rα complexes display differential signaling and functions on human hematopoietic progenitors. *Blood* **106**, 2302–2310 (2005).
16. Weber, E. W., Maus, M. V. & Mackall, C. L. The emerging landscape of immune cell therapies. *Cell* **181**, 46–62 (2020).
17. Eyquem, J. et al. Targeting a CAR to the *TRAC* locus with CRISPR/Cas9 enhances tumour rejection. *Nature* **543**, 113–117 (2017).
18. Vakulskas, C. A. et al. A high-fidelity Cas9 mutant delivered as a ribonucleoprotein complex enables efficient gene editing in human hematopoietic stem and progenitor cells. *Nat. Med.* **24**, 1216–1224 (2018).
19. Zhang, L. et al. AsCas12a ultra nuclease facilitates the rapid generation of therapeutic cell medicines. *Nat. Commun.* **12**, 3908 (2021).
20. Bulcha, J. T., Wang, Y., Ma, H., Tai, P. W. L. & Gao, G. Viral vector platforms within the gene therapy landscape. *Signal Transduct. Target. Ther.* **6**, 53 (2021).
21. Jasin, M. & Rothstein, R. Repair of strand breaks by homologous recombination. *Cold Spring Harb. Perspect. Biol.* **5**, a012740 (2013).
22. Kao, T. et al. GAPTrap: a simple expression system for pluripotent stem cells and their derivatives. *Stem Cell Rep.* **7**, 518–526 (2016).
23. Liu, Z. et al. Systematic comparison of 2A peptides for cloning multi-genes in a polycistronic vector. *Sci. Rep.* **7**, 2193 (2017).
24. Dobosy, J. R. et al. RNase H-dependent PCR (rhPCR): improved specificity and single nucleotide polymorphism detection using blocked cleavable primers. *BMC Biotechnol.* **11**, 80 (2011).
25. Park, J. B., Park, H., Son, J., Ha, S. J. & Cho, H. S. Structural study of monomethyl fumarate-bound human GAPDH. *Mol. Cells* **42**, 597–603 (2019).
26. Yilmaz, A., Peretz, M., Aharony, A., Sagi, I. & Benvenisty, N. Defining essential genes for human pluripotent stem cells by CRISPR–Cas9 screening in haploid cells. *Nat. Cell Biol.* **20**, 610–619 (2018).
27. Eisenberg, E. & Levanon, E. Y. Human housekeeping genes, revisited. *Trends Genet.* **29**, 569–574 (2013).
28. Laoharawee, K. et al. Genome engineering of primary human B cells using CRISPR/Cas9. *J. Vis. Exp.* 10.3791/61855 (2020).
29. Pomeroy, E. J. et al. A genetically engineered primary human natural killer cell platform for cancer immunotherapy. *Mol. Ther.* **28**, 52–63 (2020).
30. Robert, F., Barbeau, M., Ethier, S., Dostie, J. & Pelletier, J. Pharmacological inhibition of DNA-PK stimulates Cas9-mediated genome editing. *Genome Med.* **7**, 93 (2015).
31. Roth, T. L. et al. Reprogramming human T cell function and specificity with non-viral genome targeting. *Nature* **559**, 405–409 (2018).
32. Nguyen, D. N. et al. Polymer-stabilized Cas9 nanoparticles and modified repair templates increase genome editing efficiency. *Nat. Biotechnol.* **38**, 44–49 (2020).
33. Oh, S. A. et al. High-efficiency nonviral CRISPR/Cas9-mediated gene editing of human T cells using plasmid donor DNA. *J. Exp. Med.* **219**, e20211530 (2022).
34. Shy, B. R. et al. High-yield genome engineering in primary cells using a hybrid ssDNA repair template and small-molecule cocktails. *Nat. Biotechnol.* (2022).
35. Fennell, T. et al. CALITAS: a CRISPR–Cas-aware ALigner for In silico off-TArget Search. *CRISPR J.* **4**, 264–274 (2021).
36. Tsai, S. Q. et al. GUIDE-seq enables genome-wide profiling of off-target cleavage by CRISPR–Cas nucleases. *Nat. Biotechnol.* **33**, 187–197 (2015).
37. Kim, D. et al. Genome-wide target specificities of CRISPR RNA-guided programmable deaminases. *Nat. Biotechnol.* **35**, 475–480 (2017).
38. Kosicki, M., Tomberg, K. & Bradley, A. Repair of double-strand breaks induced by CRISPR–Cas9 leads to large deletions and complex rearrangements. *Nat. Biotechnol.* **36**, 765–771 (2018).
39. Bothmer, A. et al. Detection and modulation of DNA translocations during multi-gene genome editing in T cells. *CRISPR J.* **3**, 177–187 (2020).
40. Ivancic, D. et al. INSERT-seq enables high-resolution mapping of genomically integrated DNA using Nanopore sequencing. *Genome Biol.* **23**, 227 (2022).
41. Wang, Y., Zhao, Y., Bollas, A., Wang, Y. & Au, K. F. Nanopore sequencing technology, bioinformatics and applications. *Nat. Biotechnol.* **39**, 1348–1365 (2021).
42. Sondka, Z. et al. The COSMIC Cancer Gene Census: describing genetic dysfunction across all human cancers. *Nat. Rev. Cancer* **18**, 696–705 (2018).
43. Pickup, M., Novitskiy, S. & Moses, H. L. The roles of TGFβ in the tumour microenvironment. *Nat. Rev. Cancer* **13**, 788–799 (2013).
44. Gornalusse, G. G. et al. HLA-E-expressing pluripotent stem cells escape allogeneic responses and lysis by NK cells. *Nat. Biotechnol.* **35**, 765–772 (2017).
45. Zhang, L. et al. Author Correction: AsCas12a ultra nuclease facilitates the rapid generation of therapeutic cell medicines. *Nat. Commun.* **12**, 4500 (2021).
46. Leibowitz, M. L. et al. Chromothripsis as an on-target consequence of CRISPR–Cas9 genome editing. *Nat. Genet.* **53**, 895–905 (2021).
47. Ihry, R. J. et al. p53 inhibits CRISPR–Cas9 engineering in human pluripotent stem cells. *Nat. Med.* **24**, 939–946 (2018).
48. Keppel, M. P., Saucier, N., Mah, A. Y., Vogel, T. P. & Cooper, M. A. Activation-specific metabolic requirements for NK cell IFN-γ production. *J. Immunol.* **194**, 1954–1962 (2015).
49. Stadtmauer, E. A. et al. CRISPR-engineered T cells in patients with refractory cancer. *Science* **367**, eaba7365 (2020).
50. Ho, J. Y. et al. Promoter usage regulating the surface density of CAR molecules may modulate the kinetics of CAR-T cells in vivo. *Mol. Ther. Methods Clin. Dev.* **21**, 237–246 (2021).
51. Cichocki, F. et al. iPSC-derived NK cells maintain high cytotoxicity and enhance in vivo tumor control in concert with T cells and anti-PD-1 therapy. *Sci. Transl. Med.* **12**, eaaz5618 (2020).

Methods

Generation of plasmids, linear DNA templates and AAV6 viral preps

Plasmid constructs were synthesized by GENEWIZ. Sequences of DNA constructs are provided in the Supplementary Table. Plasmids are available upon resonable request and can be requested by contacting John Zuris at Editas Medicine. Closed-ended dsDNA linear templates were generated by GenScript. Linear dsDNA templates were cloned and linearized by Aldevron. Marker-free dsDNA circular plasmid templates using Nanoplasmid were cloned by Aldevron. ssDNA templates were generated by GenScript. AAV6 constructs were generated by Sirion Biotech.

Generation of AsCas12a protein, gRNAs and complexed RNPs

This work leverages an engineered AsCas12a containing the key M537R and F870L higher-activity mutations and demonstrating equivalent activity to the commercially available AsCas12a Ultra, which was previously described[19], and that can be purchased from Integrated DNA Technologies (IDT). In brief, DNA sequences encoding wild-type or mutant AsCas12a[19] were cloned into pET28a vector by Gibson assembly[18]. For protein expression, a single transformed *Escherichia coli* BL21(DE3) colony was inoculated into 20 ml of LB medium supplemented with 50 μg ml^{-1} kanamycin and grown overnight at 37 °C, 250 r.p.m. The overnight culture was transferred to 1 L of TB medium with kanamycin and grown at 37 °C, 250 r.p.m., for ~2–3 h until OD_{600} reached 0.6. The culture was chilled at 4 °C for 30 min before induction with 1 mM IPTG and further incubated at 18 °C, 250 r.p.m., for 12–18 h.

The recombinant AsCas12a protein was purified as previously described for SpCas9 (ref. 18). In brief, *E. coli* cells were harvested by centrifugation and homogenized with an Emulsiflex-C3 high-pressure homogenizer (Avestin). The AsCas12a protein in clarified lysate was sequentially purified using immobilized metal affinity chromatography (HisTrap HP, GE Healthcare) and heparin chromatography (HiTrap Heparin HP, GE Healthcare). Purified protein was concentrated and dialyzed overnight against storage buffer (20 mM Tris HCl, 300 mM NaCl, 0.1 mM EDTA, 50% glycerol, 1 mM DTT, pH 7.4). The protein concentration was measured by NanoDrop using extinction coefficient at 143,940 M^{-1} cm^{-1}, diluted to 60 μM and stored at −20 °C.

gRNAs were purchased from IDT using the ALT-R format and contained protospacer lengths of 21 nucleotides (nt). A list of guides used in the study is provided in the Supplementary Table. Guides and proteins were complexed at a ratio of 2:1 guide:protein to make RNP complexes and tested in cells according to procedures specific to the cell type and outlined in the 'Human primary cell culture' subsection.

Human primary cell culture

Representative flow cytometry gating strategies for iPSCs, T cells, B cells and NK cells, along with unprocessed flow cytometry plots for figures, including the fluorophore and channel labels for the given experiment, can be found in the Supplementary Information.

T cells

CD4$^+$ and CD8$^+$ T cells were isolated from peripheral blood mononuclear cells and frozen in cryopreservation media at a density of 20 × 10^6 cells per milliliter. Upon thawing, T cells were activated using anti-CD3/CD28 Dynabeads (Invitrogen) and cultured for 36 h at 1.3 × 10^6 cells per milliliter in stimulation media comprising X-VIVO 10 medium (Lonza) with 5% human serum (GeminiBio), 1.6 mg ml^{-1} *N*-acetylcysteine (MilliporeSigma), 2 mM L-alanyl-L-glutamine GlutaMAX (Thermo Fisher Scientific) and a cytokine cocktail of IL-2 at 100 IU ml^{-1} (PeproTech), IL-7 at 10 ng ml^{-1} (PeproTech) and IL-15 at 10 ng ml^{-1} (PeproTech). The Dynabeads were removed, and T cells were counted. The required number of T cells were centrifuged at 525*g* for 5 min. For electroporation, the T cells were resuspended in 20 μl of Lonza P2 or P3 buffer for AAV6 template or Lonza P3 buffer if using a non-viral template, per 0.25 × 10^6 cells. For AAV6 experiments, a total volume of 3 μl of RNP was then added prior to electroporation. For experiments using non-viral templates, a total combined volume of 3 μl of RNP and non-viral DNA template were added prior to electroporation. The cells were electroporated with CM-138 or EH-115 for AAV6 and non-viral templates, respectively, using the 96-well format Lonza 4D Nucleofector System[52]. Then, 80 μl of pre-warmed T cell stimulation media was added to the cells immediately, and the cells were plated into non-TC-treated 96-well U-bottom plates containing 100 μl of pre-warmed stimulation media. For AAV6 experiments, 1.25 × 10^{10} viral genomes per milliliter (vg ml^{-1}) of virus was added to the cells. We found that adding 2.5 μM of the DNA-PK inhibitor NU7441 (STEMCELL Technologies, 74082) at this step helps to boost HDR across all different DNA templates tested. The cells were cultured with the Dynabeads again for 48 h. The beads were then removed, and the cells were cultured in T cell expansion media (consists of X-VIVO 10 medium, human serum, *N*-acetylcysteine and L-alanyl-L-glutamine as stated above with the cytokine cocktail of IL-2 at 50 IU ml^{-1}, IL-7 at 5 ng ml^{-1} and IL-15 at 0.5 ng ml^{-1}) for an additional 5 days. KO and KI efficiencies were measured by flow cytometry or DNA sequencing methods on day 7 after electroporation unless otherwise noted.

iPSCs

The human iPSC lines were purchased from RUCDR Infinite Biologics (cell line ID: NH50191, lot numbers: R018360480 and R018496431). These iPSC lines were derived from CD34$^+$ cord blood using an episomal reprogramming method. The lines tested negative for mycoplasma contamination and positive for differentiation and have a normal XY karyotype and endogenous expression of pluripotent markers, including Oct4 and Tra-1 (shown by flow cytometry). The iPSCs were cryopreserved using Accutase and the mFreSR method. Upon thawing, iPSCs were cultured in Essential 8 Medium with supplement (Thermo Fisher Scientific) using vitronectin (1:100, Thermo Fisher Scientifc) coated flasks. iPSCs were harvested from the flasks using Accutase (Innovative Cell Technologies) and counted. The required number of cells were centrifuged at 115*g* for 5 min. The iPSCs were resuspended in 20 μl of Lonza P3 buffer per 0.1 × 10^6 cells and mixed with RNP and SLEEK KI plasmid. The cells were electroporated using the CM-138 pulse code in the 96-well format 4D Nucleofector System. Pre-warmed Essential 8 Medium supplemented with CloneR (1:10, STEMCELL Technologies) was added to the cells immediately after electroporation. The cells were plated onto vitronectin-coated 12-well plates and cultured in Essential 8 Medium supplemented with CloneR for 48 h. Thereafter, the media was refreshed daily with regular Essential 8 Medium for 5 days. Editing and KI efficiency was measured by flow cytometry on day 7 after electroporation. For iNK in vitro and animal studies, the iPSC line was obtained from BlueRock Therapeutics and edited as described above.

B cells

B cells were isolated from leukopak using CD19 positive selection and frozen in cryopreservation media at a density of 10 × 10^6 cells per milliliter. Upon thawing, the B cells were cultured in ImmunoCult B cell expansion medium (STEMCELL Technologies) for 48 h, maintaining the cell density at 5 × 10^5 cells per milliliter. The cells were counted after 2 days of thawing, and the required number of cells were centrifuged at 400*g* for 5 min. The cells were resuspended in 20 μl of Lonza P3 buffer per 1 × 10^6 cells and mixed with 3 μl of RNP. The cells were electroporated with the EO-117 pulse code using the Lonza 96-well format 4D Nucleofector System[28]. The B cells were incubated in the electroporation cuvette for 15 min at room temperature. Then, 80 μl of pre-warmed ImmunoCult medium was added to the cells, and they were placed in the tissue culture incubator for 30 min. The B cells were then plated into a 24-well plate, and AAV6 at 1.25 × 10^{10} vg ml^{-1} was added to the appropriate wells. The cells were cultured for 7 days, and media

was refreshed every 2 days to maintain the cell density at 5×10^5 cells per milliliter. Editing and KI efficiency was measured by flow cytometry on day 7 after electroporation.

NK cells

CD3-depleted NK cells were isolated from the peripheral blood mononuclear cells and frozen in cryopreservation media at a density of 50×10^6 cells per milliliter. Upon thawing, the NK cells were cultured in G-Rex plates using HDNK media consisting of X-VIVO 15 media (Lonza) with 15% heat-inactivated human serum (GeminiBio), *N*-acetylcysteine at 100 mg ml^{-1} (MilliporeSigma), L-alanyl-L-glutamine GlutaMAX at 2 mM (Thermo Fisher Scientific) and IL-15 at 5 ng ml^{-1} (PeproTech). The cell density was maintained between 1×10^6 and 1.3×10^6 cells per milliliter. On day 4 after thaw, the required number of NK cells were centrifuged at 300*g* for 5 min. The NK cells were resuspended in 20 µl of Lonza P2 buffer per 0.5×10^6 NK cells along with 3 µl of RNP. The cells were electroporated with the CM-138 pulse code using the Lonza 96-well format 4D Nucleofector System. Then, 80 µl of pre-warmed NK cell media was added to the cells immediately, and the cells were plated into non-TC-treated 96-well U-bottom plates. For AAV6 experiments, the virus at 1.25×10^{10} vg ml^{-1} was added to the cells. Then, 2.5 µM of the DNA-PK inhibitor NU7441 (STEMCELL Technologies, 74082) was added to the cells to further increase HDR. Cells were washed, and media was changed after 48 h. The cells were cultured for five more days and analyzed by flow cytometry on day 7 after electroporation.

iPSC differentiation to iNK cells

iPSC cells were cultured for 7 days in E8 media (Thermo Fisher Scientific) before forming embryoid bodies (EBs). EBs were generated by the spin EB method[53]. In brief, iPSCs were harvested from their culture vessel with gentle cells dissociation reagent (GCDR) (STEMCELL Technologies) for 5–8 min. Cells were then resuspended in E8 media and centrifuged at 234*g* for 5 min. After the spin, cells were resuspended in APEL2 (STEMCELL Technologies) differentiation media, which consisted of 40 ng ml^{-1} SCF, 20 ng ml^{-1} VEGF, 20 ng ml^{-1} BMP4 and 10 µM ROCK inhibitor. Cytokines were purchased from PeproTech, and ROCK inhibitor was purchased from STEMCELL Technologies. Cells were then counted using trypan blue staining. In total, 6,000 cells per well of a 96-well ultra-low attachment plate (Corning) were seeded. Once the plate was seeded, it was spun down at 234*g* for 5 min. On days 3, 6 and 9 after EB formation, 65 µl of APEL2 differentiation media, the same media configuration as described above, was added to all the wells. On day 11 after EB formation, EBs were harvested from the 96-well plates and seeded into either T-25 or T-75 flasks. To harvest EBs, wide-bore P1000 tips were used. EBs were then placed into 25-ml reservoirs and then placed into 50-ml conical tubes. EBs were allowed to gravity settle; once settled at the bottom, the media was replaced with NK MACS (Miltenyi Biotec). The composition of the NK MACS media was NK MACS basal media with supplement, 5 ng ml^{-1} IL-3, 20 ng ml^{-1} IL-7, 10 ng ml^{-1} IL-15, 20 ng ml^{-1} SCF, 10 ng ml^{-1} FLT3L and 15% human serum. IL-3 is only required in the first week of differentiation, and then it is removed from the media. Media was changed twice a week, and cell counts and phenotype were monitored throughout the culture period.

Flow cytometry

Cells were centrifuged at 234*g* for 5 min, resuspended in DPBS containing appropriate stains, incubated at 4 °C for 30 min and washed and resuspended in DPBS for flow cytometry. Staining consisted of the following antibodies: APC anti-human HLA-A/B/C (BioLegend, clone W6/3, 1:100 dilution), BV421 anti-human TCR-α/β (BioLegend, clone IP26, 1:100 dilution), FITC-labeled human CD19 protein (ACROBiosystems, 1:100 dilution), PE anti-human HLA-E (BioLegend, clone 3D12, 1:100 dilution), PerCP/Cyanine5.5 anti-human CD16 (BioLegend, clone 3G8, 1:50 dilution), BV786 mouse anti-human CD215 (IL-15Rα) (BD Biosciences, clone JM7A4, 1:16 diltuion), PE/Dazzle 594 anti-human CD3 (BioLegend, clone UCHT1, 1:100 dilution), PE/Cyanine 7 anti-human CD19 (BioLegend, clone SJ25C1, 1:100 dilution), biotinylated recombinant human EGFR protein (Sino Biological, 1:100 dilution), PE anti-human CD107a (BD Biosciences, clone H4A3, 1:40 dilution) and streptavidin-FITC (BioLegend, 1:200 dilution). Data were acquired using the NovoCyte Quanteon (Agilent Technologies) using NovoExpress 1.5.6 software and later analyzed using FlowJo version 10.8.1.

Genomic DNA extraction

For primary cells (T cells, iPSCs, iNK cells and HDNK cells), genomic DNA (gDNA) was isolated using the Agencourt DNAdvance Kit (Beckman Coulter) according to the manufacturer's instructions and quantified using Quant-iT PicoGreen dsDNA Assay Kit (Thermo Fisher Scientific).

ddPCR

ddPCR assays were used to determine the targeted integration at *GAPDH* locus. ddPCR primers and probes targeting a specific region in the gDNA after KI at *GAPDH* were designed using Primer3 or Geneious software. Primers and probes for targeted integration at *GAPDH* were ordered from IDT. ID1 gene primer and probes were ordered from Bio-Rad. ddPCR reactions were made according to the following table using Bio-Rad ddPCR Supermix for probes (no dUTP), 900 µM of primers and 250 nM of probes for both target and reference sequences and 15 ng of gDNA per reaction. The reactions were performed in triplicate per integration primer/probe set. Droplets were generated on Bio-Rad AutoDG system and then placed in the thermocyclers. After amplification, the plates were transferred to the Bio-Rad ddPCR Reader for analysis. Integration frequency was determined as the ratio of target gene copy numbers compared to the reference gene copy numbers, with gene copy number being calculated by Bio-Rad's QuantaSoft software. Replicates with fewer than 10,000 accepted droplets were discarded, and the remaining datasets were then averaged together for a final integration rate. The list of sequences for ddPCR primers and probes used in the study is provided in the Supplementary Table.

Translocation detection assays

Translocation rates were measured using ddPCR according to previously described methods[39]. In brief, translocation junctions were modeled in Geneious based on gRNA cut sites among *TRAC*, *B2M* and *GAPDH*. ddPCR primers and probes targeting flanking regions around the translocation junction were designed using Primer3. Amplicon sizes ranged from 400 bp to 600 bp in length, and melting temperatures for all primer/probe combinations were selected for ~58 °C. Each permutation of translocation was ascertained with individual ddPCR reactions within the same assay. The permutations of translocations involving the homologous fragment of each gene of interest could not be assessed due to aggressive hairpin formation, interfering with the PCR. Primer sequences for ddPCR-based translocation measurements used in this study are provided in the Supplementary Table.

RT–qPCR

Cellular total RNA was extracted from 1 million iPSCs or iNK cells per sample using a RNeasy Kit (Qiagen). Total RNA was measured spectrophotometrically using a Thermo Fisher Scientific NanoDrop spectrometer for purity and concentration. The samples were diluted to 20 ng $µl^{-1}$ and then converted to cDNA using a SuperScript IV VILO Master Mix (Invitrogen) on a Veriti 96 thermocycler (Applied Biosystems). cDNA negative controls that lacked reverse transcriptase were also generated for each sample. To perform the RT–PCR, 4 ng of cDNA was prepared with a TaqMan Fast Gene Expression Master Mix (Thermo Fisher Scientific) and TaqMan probes from Thermo Fisher Scientific for TBP and GADPH standards. The prepared samples were run in a QuantStudio Real-Time PCR System (Thermo Fisher Scientific)

and analyzed using QuantStudio Real-Time PCR System analysis software. Cycle threshold (CT) values were obtained and converted to fold expression using TBP as a reference for all samples.

H2AX and p53 phosphorylation ELISA assays

Both unedited or SLEEK-edited T cells allowed to expand for 7 days or 14 days were isolated and then lysed in ice-cold Cell Lysis Buffer (Cell Signaling Technology). DNA damage was assessed by measuring phosphorylation of p53 and H2AX at serine 15 and 139, respectively, with PathScan Phospho-Histone H2A.X (Ser139) and Phospho-p53 (Ser15) Sandwich ELISAs as per the manufacturer's protocol.

In vitro tumor killing assays

Cytotoxicity of T cells and NK cells was evaluated using a lactate dehydrogenase (LDH) cytotoxicity assay[54] (CyQUANT detection kit, Invitrogen, C20300) or a DELFIA time-resolved fluorescence (TRF) cytotoxicity assay (PerkinElmer, AD0116) or a 3D SKOV-3 tumor spheroid assay. Target cell lines used in killing assays included NALM6 (American Type Culture Collection (ATCC), CRL-3273), Raji (ATCC, CCL-86) and SKOV3 (ATCC, HTB-77). All cell lines were maintained according to the manufacturer's recommendations. In brief, cells cryopreserved in CryoStor CS10 (STEMCELL Technologies, 07930) at 5×10^6 cells per milliliter were thawed using a 37 °C water bath and plated in RPMI 1640 medium (Gibco, 11875085) with 10% FBS (Gibco, A4766801) at a density of 6.25×10^4 cells per milliliter (Raji, NALM6) or 1.5×10^5 cells per cm^2 (SKOV3). Complete media changes were performed every other day, and subculturing to readjust density to 6.25×10^4 cells per milliliter was performed weekly. Cells used in assays were maintained in culture for no longer than 8 weeks.

For the LDH assay, target cells were resuspended in assay media (RMPI 1640 with 10% FBS) at a density of 1×10^5 cells per milliliter. Then, 5×10^3 tumor cells in 50 µl of assay media were added to each well of either a U-bottom 96-well plate (Raji, NALM6) or a flat-bottom tissue culture-treated 96-well plate (SKOV3). Effector cells were re-suspended in 50 µl of assay media at densities calculated to produce desired E:T ratios and were added to target cells for a total reaction volume of 100 µl per well. Maximum LDH released by 5×10^3 target cells were evaluated by adding 5 µl of lysis buffer (component of the CyQUANT kit, warmed to 37 °C) to 50 µl of target cells and adjusting the total volume to 100 µl with assay media. Spontaneous LDH release by target cells was evaluated by adding 50 µl of assay media to 50 µl of target cells. Wells were gently centrifuged at 125*g* for 2 min and then incubated at 37 °C for 24 h. Quantification of LDH release using the CyQUANT kit was performed according to manufacturer recommendations. After 24 h of co-culture, 50 µl of supernatant was combined with 50 µl of Reaction Mixture (component of the CyQUANT kit, warmed to room temperature) in a black flat-bottom 96-well plate and incubated for 30 min at room temperature in the dark. Then, 50 µl of Stop Solution (component of the CyQUANT kit, warmed to room temperature) was added to each well; well contents were mixed by gently tapping the edges of the plate to avoid introduction of bubbles. Released LDH was detected using an EnVision plate reader (PerkinElmer) with excitation of 560 nm and emission of 590 nm. Relative cytotoxicity was reported as relative fluorescence units (RFUs) with RFUs of spontaneous and lysis-buffer-induced LDH released presented for comparison.

For the DELFIA assay[55], NALM6 cells were resuspended at a density of 1×10^5 cells per milliliter in assay media containing BATDA ligand (component of the DELFIA kit) diluted 1:500. Cells were incubated with BATDA ligand (component of the DELFIA kit) at 37 °C for 40 min and then washed 3× by resuspending in 10 ml of assay media, centrifuging at 234*g* for 5 min and aspirating the supernatant. BATDA-loaded target cells were resuspended in assay media at a density of 2.5×10^5 cells per milliliter, and 2.5×10^4 tumor cells in 100 µl of assay media were added to each well of a U-bottom 96-well plate. Effector cells were re-suspended in 100 µl of assay media at densities calculated to produce desired E:T ratios and were added to target cells for a total reaction volume of 200 µl per well. Maximum BATDA ligand released from 2.5×10^4 target cells was evaluated by adding 10 µl of lysis buffer (component of the DELFIA kit, warmed to 37 °C) to 100 ul of target cells and adjusting the total volume to 200 µl with assay media. Spontaneous LDH released by target cells was evaluated by adding 100 µl of assay media to 100 µl of target cells. Wells were gently centrifuged at 125*g* for 2 min and then incubated at 37 °C for 2 h. Quantification of BATDA ligand release was performed according to manufacturer recommendations. After 2 h of co-culture, 20 µl of supernatant was combined with 200 µl of europium solution and incubated on a plate rocker in the dark for 20 min. Released BATDA ligand was detected using an EnVision time-resolved fluorometer. Relative cytotoxicity is reported as RFUs with RFUs of spontaneous and lysis-buffer-induced LDH release presented for comparison.

For the 3D tumor spheroid assay, SKOV-3 cells were transduced with NucLight Red Lentivirus (Sartorius, 4476) and sorted for positive expression (data not shown). To perform 3D killing assays, 5×10^3 NucLight Red-transduced SKOV-3 cells were plated in 100 µl of assay media into U-bottom ULA 96-well plates (Corning, 7007). Plates were centrifuged at 234*g* for 10 min to pellet cells and then incubated at 37 °C for 96 h to form spheroids (one per well). Trastuzumab was added to 50 µl of media to achieve a final concentration of 10 µg ml^{-1} in 200 µl of assay volume. Effector cells were resuspended in assay media at 3.16×10^6 cells per milliliter, and seven serial dilutions were made to cover an eight-point, half-log concentration curve. Effector cells at each concentration were gently added to the SKOV-3 spheroids in technical duplicates. Plates were immediately transferred to an Incucyte S3 Live-Cell Analysis Instrument (Sartorius). Images were collected at 2-h intervals for 100 h, and Total Integrated Red Object Intensity values were exported for downstream analysis. Normalized spheroid size, calculated as the ratio of total integrated red object intensity at 100 h and 0 h, was plotted against E:T ratio. A nonlinear regression was fit to the data, and the resulting curve was used to determine an absolute IC_{50}.

CellTiter-Glo assay

SLEEK DKI and unedited iNK cells were seeded starting at 5×10^4 cells and serially diluted down to 3,175 cells per well in a white solid-bottom 96-well plate in 50 µl of culture media. Then, 50 µl of pre-mixed CellTiter-Glo was added to each well, after which the plates were kept at room temperature in a dark space for 10 min to allow for cell lysis. RLUs were then measured using the PerkinElmer EnVision plate reader.

For iPSC cells, 2.5×10^4 cells were seeded into laminin-521-coated six-well plates. These cells were grown for 6 days, with media being changed every day. On the sixth day, media was removed from the wells. Cells were washed with 1 ml of DPBS. Then, 1 ml of DBPS and 1 ml of pre-mixed CellTiter-Glo were added to each well, after which the plates were put into a dark space at room temperature for 10 min to allow for cell lysis. Three samples were taken from each well of the six-well plates and plated into a white solid-bottom 96-well plate. RLUs were then measured using the PerkinElmer EnVision plate reader.

Degranulation assay for assessing NK cell lysis inhibition

HDNK cells and T cells were cultured as described previously[19] for use in a degranulation assay[44]. HDNK cells and T cells were pelleted by centrifuging at 525*g* for 10 min. HDNK cells were resuspended in RPMI with 10% FBS, non-essential amino acids and GlutaMAX. T cells were resuspended in 500 µl of PBS, and an additional 500 µl of PBS with a 2× solution of CFSE stain was added. T cells were allowed to incubate for 3 min. To wash the CFSE, 9 ml of RPMI media was added, and the cells were centrifuged at 525*g* for 10 min. HDNK cells and T cells were counted using an AO/PI dye and adjusted to 5×10^5 cells in 50 µl. HDNK cells and T cells were then mixed at a 1:1 ratio—50 µl of both HDNK cells and T cells into one well of a 96-well plate. Then, 2.5 µl of an anti-CD107a antibody was added to each well along with 5 µl of GolgiStop into each

well. Reactions were then incubated overnight, and cells were analyzed by flow cytometry.

Metabolism assays to assess effect of SLEEK KI at *GAPDH* locus

For both iPSC and iNK flow-cytometry-based measurements, 1×10^5 cells were aliquoted into wells of a 96-well plate. Cells were washed with DPBS and spun down at 234*g* for 5 min. For GLUT1 (Abcam, ab195359) surface expression, cells were brought back up in 100 µl of DPBS with 10% Fc Block. Then, 2 µl of antibody was added to the appropriate well. Cells were incubated at 4 °C for 30 min, after which they were again washed with DPBS and centrifuged at 234*g* for 5 min. The cells were resuspended in 100 µl of DPBS and analyzed on the Quanteon flow cytometer. The following intracellular antibodies were used at a 1:50 dilution: ACAC (Abcam, ab109368), CPT1A (Abcam, ab171449), IDH2 (Abcam, ab212122), G6PD (Abcam, ab133525), ASS1 (Abcam, ab210451), PRDX2 (Abcam, ab197536) and ATP5A (Abcam, ab196198). For these samples, after washing, the cells were fixed and permeabilized using the BD Cytofix/Cytoperm reagent (BD Biosciences, 554714). Samples were incubated for 20 min at room temperature and then washed with Perm Wash and centrifuged again at 234*g* for 5 min. Samples were resuspended in Perm Wash with the appropriate antibody and incubated at 4 °C for 30 min. Samples were then again washed with Perm Wash. Samples stained with conjugated antibodies were then resuspended with DPBS and analyzed on the Quanteon. Samples stained with unconjugated antibodies were then stained 1:200 with Alexa Fluor 647 (Thermo Fisher Scientific, A-21445) in Perm Wash for 20 min. Samples washed with Perm Wash were then resuspended with DPBS and analyzed on the Quanteon.

To analyze glucose consumption, which was assessed by directly measuring lactate concentrations, SLEEK DKI and unedited iPSCs were seeded at a target density of ~15,000–20,000 live cells per cm^2 on laminin-coated, tissue-culture-treated T-flasks. Cells were cultured in Essential 8TM Medium (Gibco, A1517001) at 37 °C for 3–4 days. Y-27632 ROCK inhibitor (Tocris, TB1254-GMP) was added at 0.01 mM during inoculation to promote iPSC survival. Cultures were subsequently fed daily via 100% exchange of the spent media. Media samples were taken during routine medium exchanges to determine glucose and lactate concentrations. Then, 0.5–1-ml samples were transferred to 1.5-ml Eppendorf tubes and analyzed on the BioProfile FLEX2 (Nova Biomedical) using the electrochemical biosensors on the chemistry cartridge.

Western blot analysis on GAPDH and CD16 proteins

Unedited and SLEEK DKI IPSCs were lysed in 500 µl of ice-cold RIPA buffer (Thermo Fisher Scientific) containing protease inhibitors (Roche). The lysate was centrifuged at 4 °C, and the supernatant was separated from the pellet and stored at −80 °C. The supernatant was thawed on ice, and protein concentration was determined using the Pierce 660-nm Protein Assay Kit (Pierce Biotechnology). Protein samples were separated under reducing conditions on NuPage 4–12% Bis-Tris Gel (Invitrogen), transferred to a blot using the iBlot 2 Dry Blotting System and analyzed by western blotting using primary antibodies rabbit polyclonal anti-beta tubulin (Novus Biologicals, 1:5,000 dilution) and mouse monoclonal anti-GAPDH (Cell Signaling Technology, 1:1,000 dilution), followed by secondary antibodies anti-mouse HRP (Invitrogen, 1:5,000 dilution) and goat anti-rabbit IgG, HRP (Invitrogen, 1:5,000 dilution). Blots were incubated with chemiluminescent substrate (Thermo Fisher Scientific) and imaged with a Bio-Rad ChemiDoc MP Imaging System. The same blot was then analyzed with the primary antibody rabbit monoclonal anti-CD16 (Cell Signaling Technology, 1:1,000 dilution) and the secondary antibody goat anti-rabbit IgG, HRP (Invitrogen, 1:5,000 dilution).

Animal studies

Animal studies were performed in compliance with animal guidelines and protocols approved by the Institutional Animal Care and Use Committee at the Charles River Accelerator and Development Lab (CRADL) under protocol number CR-0058. Six-week-old female non-obese diabetic (NOD) severe combined immunodeficient (SCID) gamma (NSG) mice were purchased from The Jackson Laboratory (005557) and maintained in pathogen-free conditions at CRADL. Mice were housed under dark and light cycles of 12 h. The average temperature was 21 °C with fluctuations ranging from 20 °C to 26 °C. Relative humidity averaged 60% and did not exceed 70% or fall below 30%. NSG mice were IP inoculated with $0.25–1.00 \times 10^6$ luciferase-expressing SKOV-3 cell line (SKOV-3-luc) ovarian tumor cells. Three days after tumor inoculation, mice were assessed for tumor engraftment using BLI and randomized into groups with similar tumor burden ($n = 8$ per treatment group). Treatment was initiated on day 4 when tumor-bearing mice were treated IP with a single dose of 5×10^6 unedited iNK cells or SLEEK DKI iNK cells in combination with a single IP dose of 2.5 mg kg^{-1} trastuzumab . No exogenous IL-2 or IL-15 cytokine treatment was provided. Tumor burden was calculated using a PerkinElmer bioluminescent IVIS. For BLI, mice were injected with D-luciferin at 10 µl g^{-1} of body weight, so that each mouse received 150 mg of luciferin per kilogram of body weight. Mice were anesthetized using isoflurane and imaged 10 min later. Bioluminescent images were collected once a week throughout the duration of the study. Animals were monitored twice weekly for normal activity, and survival endpoints included poor body conditions (that is, ascites) and a tumor burden BLI > 10^{11}. Mice were sacrificed at the endpoint to assess iNK persistence and CD16 expression in the peritoneal cavity by flow cytometry. Lungs were collected and inflated with 10% neutral buffered formalin and fixed in the same fixative for 30 h for immunohistochemistry analysis.

Immunohistochemistry analysis

Lungs were processed for paraffin embedding. Her2 immunostaining was performed in 5-µm paraffin sections with BOND RX Stainer. In brief, heat-mediated antigen retrieval was performed using citrate buffer (pH 6.0, epitope retrieval solution 1) for 20 min after de-waxing and rehydration. The primary rabbit anti-Her2 antibody (Abcam, ab16662, 1:1,000) was used for detection of Her2-positive tumor cells. BOND Polymer Refine Kit (Leica, DS9800) was applied as the detection system. The positive cells were identified as brown in color by DAB, and nuclei were stained blue with hematoxylin as counterstain. The stained slides were scanned with a P250 scanner from 3DHISTECH; the whole digital slides were reviewed; and representative images were taken using SlideViewer software.

Selection of SLEEK gRNAs

AsCas12a guides targeting essential genes were selected using a specific set of criteria. Essential genes were chosen from a pool of potential sites made by intersecting the essential genes described by Yilmaz et al.[26] and by Eisenberg et al.[27]. In brief, the list of essential genes for human pluripotent stem cells with CRISPR scores less than 0 and false discovery rate (FDR) < 0.05 (ref. 26) was intersected with the list of human housekeeping genes that are expressed uniformly across a panel of tissues[27], resulting in a set of 907 essential genes. These genes were then sorted by their average expression level (mean transcripts per million (TPM) across different tissues using Protein Atlas data; see, for example, RNA consensus tissue gene expression data provided by https://www.proteinatlas.org/ (ref. 56)). Potential gRNA target sequences were identified by searching for AsCas12a-specific PAM sites (TTTV) with suitable protospacers mapped to the final last exon of a representative coding region of those putative essential genes in the human reference genome (hg38). Transcripts with their name followed by '-201' were selected as the representative for each gene (for example, GAPDH-201). Gene information (that is, coding region) was obtained from GENCODE version 37 gene annotation GTF file. For the transcripts with large final exon (>500 bp), only the gRNAs cutting within 500 bp to the stop codon were retained. Finally, the retained gRNAs were aligned

to the human reference genome (for example, hg38) with CALITAS, and those non-specific guides aligned to multiple genomic locations with fewer than two mismatches and gaps were filtered out[35].

Quantification of genome editing by NGS

For measuring on-target editing, round 1 PCR was performed in a 12-µl reaction volume, consisting of 6 µl of NEBNext Ultra II Q5 Master Mix (New England Biolabs), 0.25 µM forward and reverse primer and 20 ng of gDNA template. PCR conditions were as follows: 30 s at 98 °C for initial denaturation, followed by 20 cycles of 10 s at 98 °C for denaturation, 15 s at 60 °C for annealing, 30 s at 72 °C for extension and 5 min at 72 °C for the final extension. Round 2 PCR was performed in a 12-µl reaction volume, consisting of 6 µl of NEBNext Ultra II Q5 Master Mix (New England Biolabs), 1 µM forward and reverse primers and 4 µl of PCR round 1 product. PCR conditions were as follows: 30 s at 98 °C for initial denaturation, followed by 14 cycles of 10 s at 98 °C for denaturation, 15 s at 60 °C for annealing, 30 s at 72 °C for extension and 5 min at 72 °C for the final extension. The PCR reactions that were to be combined into a sequencing library were pooled and purified using AMPure XP beads (Beckman Coulter) as per the manufacturer's protocol. Purified products were size-selected in the 300–1,200 bp range using a BluePippin (Sage Science) and re-purified with AMPure XP beads (Beckman Coulter). Then, 8–10 pmol of sequencing library was analyzed using MiSeq Reagent Kit version 3 with 10–15% PhiX Control version 3 (Illumina) to obtain 2 × 300 cycle reads. Source code and data analytical methods are as described in Maeder et al.[57].

Three orthogonal approaches were performed—CALITAS[35], GUIDE-Seq[36] and Digenome-Seq[37]—to identify potential off-targets. Digenome-Seq and GUIDE-Seq experiments were performed as described in Maeder et al.[57]. The *GAPDH* SLEEK RNP targets a position in the genome denoted as chr12:6538091–6538112 (DNA protospacer: 5′-ATCTTCTAGGTATGACAACGA-3′). In total, 477 unique, non-redundant candidate sites were identified by the discovery phase studies (457 from CALITAS, 22 from Digenome-Seq and zero from GUIDE-Seq, with two targets found in common to CALITAS and Digenome-Seq). Off-target verification was achieved by taking gDNA extracted from $CD8^+$ T cells treated with the SLEEK RNP which showed 97% on-target editing at the *GAPDH* site by NGS.

To verify potential off-targets, rhAmpSeq was performed, and primers for the off-target detection assay were designed as described previously[24]. In brief, multiplex amplicons were designed, and DNA primers were ordered through the IDT website (https://www.idtdna.com/pages/tools/rhampseq-design-tool), using a minimum insert size of 70 bp and a maximum insert size of 200 bp and limiting the number of amplicons in a pool to 200. Round 1 PCR was performed in a 20-µl reaction volume, consisting of 5 µl of 4× rhAmpSeq Library Mix 1 (IDT), 20 ng of gDNA template, 2 µl each of 10× forward and reverse rhAmpSeq Index Primer pools and nuclease-free water. PCR conditions were as follows: 10 min at 95 °C for initial denaturation, followed by 10 cycles of 15 s at 95 °C for denaturation, 4 min at 61 °C for annealing and extension and a final 15 min at 99.5 °C for enzyme inactivation. The PCR product was purified using (1.5×) Agencourt AMPure XP beads (Beckman Coulter Agencourt AMPure XP, PCR Purification, A63882) as per the manufacturer's protocol and eluted in 15 µl of Low TE (10 mM Tris, pH 8.0, 0.1 mM EDTA, Quality Biological, 351-324-721). Round 2 was performed in a 20-µl reaction volume, consisting of 5 µl of 4× rhAmpSeq Library Mix 2 (IDT), 0.5 µM forward and reverse round 2 PCR primers and 11 µl of round 1 PCR product. PCR conditions were as follows: 3 min at 95 °C for enzyme activation, followed by 18 cycles of 15 s at 95 °C for denaturation, 30 s at 60 °C for annealing, 30 s at 72 °C for extension and 1 min at 72 °C for the final extension. The PCR product was purified using (1×) Agencourt AMPure XP beads (Beckman Coulter Agencourt AMPure XP, PCR Purification, A63882) as per the manufacturer's protocol except for the use of freshly prepared 80% ethanol for washing. PCR product was eluted in 20 µl of Low TE. The final sequencing libraries were loaded at 8 pM on an Illumina MiSeq Flow Cell Kit version 2 with 10% PhiX Control version 3 (Illumina, FC-110-3001) using a 2 × 150-bp paired-end read sequencing configuration with 8-bp dual index reads. Analysis of indel rates was performed as described previously[39], with the difference that reads were aligned to a reference FASTA file containing all rhAmpSeq amplicons included in the panel. In brief, paired-end reads were first merged using PEAR version 0.9.6 (ref. 58). Merged reads were aligned using bowtie2 version 2.4.4 (ref. 59). Quantification of insertions and deletions overlapping a 2-bp window around the expected cut site in each amplicon was done by parsing the cigar string using SAMtools version 1.13 (ref. 60).

ONT long-read sequencing

gDNA was extracted from samples using the NucleoBond HMW DNA Kit (Takara, 740160.20) according to the enzymatic lysis protocol, section 5.1 of the manual. In brief, the cell pellets were incubated with proteinase K and H1 lysis buffer for 30 min at 50 °C. RNA was digested with the addition of RNase A at room temperature for 5 min. The filters and columns were first equilibrated by adding 12 ml of H2 buffer, and the flow-through was discarded. Then, the samples mixed with 10 ml of H2 buffer were loaded onto the column filters to bind the DNA, and the flow-through was discarded. The column filters were flushed out by adding 6 ml of H3 buffer. Once the buffer had gone through the columns, the flow-through and the filter were discarded. The columns were washed with 12 ml of the H4 buffer, and the flow-through was discarded. The columns were transferred to a new 50-ml conical tube, and the DNA was eluted with 5 ml of the H5 buffer. Next, the DNA was precipitated with 3.5 ml of isopropanol, mixed by inverting and centrifuged at room temperature for 10 min at 4,500*g*. The pellet was washed with 2 ml of 70% ethanol and centrifuged at room temperature for 5 min at 4,500*g*. The supernatant was discarded, and the pellet was dried at room temperature until no ethanol drops were visible. The gDNA was resuspended in 100 µl of HE resuspension buffer. After elution, the DNA was quantified with the NanoDrop, with the Qubit Broad Range dsDNA Assay and on the Agilent 4200 Genomic DNA TapeStation.

gDNA samples were processed using the ONT Cas9 targeted sequencing kit (SQK-CS9109). In brief, 5 µg of gDNA was first dephosphorylated and incubated on a thermal cycler at 37 °C for 10 min and 80 °C for 2 min and held at 20 °C (room tempterature). Then, Taq polymerase, dATPs and Cas9 RNPs were added to the reaction to cut and dA-tail the dephosphorylated gDNA. The reaction was incubated at 37 °C for 20 min, followed by 72 °C for 5 min and then held at 4 °C before proceeding to adapter ligation. For adapter ligation, ligation buffer (LNB), nuclease-free water, T4 DNA ligase and adapter mix (AMX) were mixed and then added to the cleaved and dA-tailed DNA. The reaction was incubated for 10 min at room temperature. The reaction was cleaned up with 0.3× volume of AMPure XP beads, washed with long fragment buffer (LFB) and eluted in 13 µl of elution buffer. The sample was loaded onto the flow cell according to the manual and run for 24 h on the GridION.

Editing statistics were obtained by a series of steps using publicly available tools. Reads from the samples were first aligned with Minimap2 version 2.24-r1122 (ref. 61) against both an hg38 genome and a custom reference consisting of a wild-type and expected insertion sequence. The wild-type sequence was generated by taking 20,000 bases from the hg38 reference centered around the cut site at position chr12:6,538,112, and the insertion sequence was generated using the same region but with the addition of the expected plasmid cargo after editing. The custom reference-aligned reads were then filtered using pysam version 0.19.1 (a Python wrapper to SAMtools version 1.16.1 (ref. 60)) to remove highly clipped (>95%) and low alignment score reads, with alignment score normalized against the read length ((alignment score / read length) < 0.20). The aligned reads from both the hg38 and custom reference alignments were then processed using a Python script to quantify mapping rates to the target regions. This script parsed each read for multi-mapping sites between the target region and other genomic regions, which can be a predictor of off-target

insertion, as well as for overlapped multi-mapping sites within the target region, which can indicate incorrect insertion at the target. To quantify editing and insertion efficacy, the script also examined the cut site position in the wild-type custom reference alignment for evidence of editing, which was taken as the presence of an indel at chr12:6,538,112 larger than 5 bp and categorized as 'indel', as well as examining the expected insertion alignment for indels within the insertion sequence. Any indel larger than 10 bp within the insertion sequence or 50 bp 5′ or 3′ of the insertion sequence was considered as affecting expression and categorized as 'incorrect cargo insertion'. If the insertion did not have any indel larger than 10 bp within the insertion sequence or 50 bp 5′ or 3′ of the insertion sequence, it was considered a 'correct cargo insertion'; this includes multiple-cargo insertions for which the first cargo is correctly inserted without indels. Reads were then filtered for primary mapped reads that had a mapping quality over 2 and which intersected the cut site. These counts were used for calculating mapping rates. Editing categories were defined as follows: Unedited—no indel or cargo inserted at *GAPDH* allele; Correct Cargo Insertion—cargo is inserted in frame, and *GAPDH* final exon is restored; Incorrect Cargo Insertion—cargo may be inserted, but there are indels larger than 10 bp within the cargo sequence or 50 bp 5′ or 3′ of the insertion, preventing proper expression of *GAPDH* or transgene; and Indels—insertion or deletion without cargo larger than 5 bp at chr12:6,538,112.

Statistical analysis

Quantitative assays were performed in technical and/or biological replicates, with replicate number indicated in the figure legends. To determine statistical significance, unpaired *t*-tests and one-way or two-way ANOVAs with Tukey's post hoc test were calculated in GraphPad Prism 9.5.1. Statistically significant comparisons with $P < 0.05$ are indicated in each figure and legend, and comparisons with $P > 0.05$ were considered non-significant.

Reporting summary

Further information on research design is available in the Nature Portfolio Reporting Summary linked to this article.

Data availability

Source data are provided with this paper. Unprocessed flow cytometry and microscopy images for Figs. 1–5 are provided as Source Data File 1, and numerical values for plotted data in Figs. 1–5 are provided as Source Data File 2. DNA constructs, gRNAs, primers, ddPCR probes, Digenome-Seq results and rhAmp-Seq panel of potential off-target candidate sites are listed in the Supplementary Table. All numerical data values used to generate figures in the Supplementary Information can be found in Supplementary Data. Raw flow cytometry plots and representative gating strategies, as well as uncropped microscopy and gel images, are provided in the Supplementary Information under Supplementary Notes. High-throughput sequencing data have been deposited in the National Center for Biotechnology Information's Sequence Read Archive database (accession code PRJNA947757) and can be found at http://www.ncbi.nlm.nih.gov/bioproject/947757 (ref. 62). Source data are provided with this paper.

Code availability

Custom code used to analyze Digenome-Seq data is available at the Editas Medicine GitHub page at https://github.com/editasmedicine/digenomitas. Custom code used to identify candidate in silico off-target sites is also available at the Editas Medicine GitHub (https://github.com/editasmedicine/calitas).

References

52. Kath, J. et al. Pharmacological interventions enhance virus-free generation of *TRAC*-replaced CAR T cells. *Mol. Ther. Methods Clin. Dev.* **25**, 311–330 (2022).
53. Ng, E. S., Davis, R. P., Azzola, L., Stanley, E. G. & Elefanty, A. G. Forced aggregation of defined numbers of human embryonic stem cells into embryoid bodies fosters robust, reproducible hematopoietic differentiation. *Blood* **106**, 1601–1603 (2005).
54. Decker, T. & Lohmann-Matthes, M. L. A quick and simple method for the quantitation of lactate dehydrogenase release in measurements of cellular cytotoxicity and tumor necrosis factor (TNF) activity. *J. Immunol. Methods* **115**, 61–69 (1988).
55. Allicotti, G., Borras, E. & Pinilla, C. A time-resolved fluorescence immunoassay (DELFIA) increases the sensitivity of antigen-driven cytokine detection. *J. Immunoassay Immunochem.* **24**, 345–358 (2003).
56. Uhlen, M. et al. Proteomics. Tissue-based map of the human proteome. *Science* **347**, 1260419 (2015).
57. Maeder, M. L. et al. Development of a gene-editing approach to restore vision loss in Leber congenital amaurosis type 10. *Nat. Med.* **25**, 229–233 (2019).
58. Zhang, J., Kobert, K., Flouri, T. & Stamatakis, A. PEAR: a fast and accurate Illumina Paired-End reAd mergeR. *Bioinformatics* **30**, 614–620 (2014).
59. Langmead, B. & Salzberg, S. L. Fast gapped-read alignment with Bowtie 2. *Nat. Methods* **9**, 357–359 (2012).
60. Li, H. et al. The Sequence Alignment/Map format and SAMtools. *Bioinformatics* **25**, 2078–2079 (2009).
61. Li, H. Minimap2: pairwise alignment for nucleotide sequences. *Bioinformatics* **34**, 3094–3100 (2018).
62. Marco, E. A highly efficient transgene knock-in technology in clinically relevant cell types. National Center for Biotechnology Information. http://www.ncbi.nlm.nih.gov/bioproject/947757 (2023).

Acknowledgements

We would like to thank additional members of the Editas Computational Biology, Informatics and Sequencing groups for generation and pipeline analysis of sequencing data. We thank R. Naines, C. Wang, J. Yao and H. An for providing primary cells for studies. We would like to thank J. Getgano, K. Gareau, E. Goncz, S. Zhang, J. Moon, K. Tsiounis and J. Schafer for support in the development of key assays and protocols. We would like to thank members of BlueRock Therapeutics LP for their support and collaboration related to engineering and culturing iPSCs. We would like to thank A. Dee for paper preparation support. Several graphics in the figures (cells in Fig. 1a, cells in Fig. 2a,h, cells in Fig. 3a,d,g, mouse schematic in Fig. 5a, cells in Supplementary Fig. 5c, cells in Supplementary Fig. 9c,e, cells in Supplementary Fig. 10a, cells in Supplementary Fig. 11a–c, cells in Supplementary Fig. 12c, cells in Supplementary Fig. 13a and cells in Supplementary Fig. 14a,b) were created with BioRender. We would like to thank Porterhouse Medical for graphic design support.

Author contributions

A.G.A, S.Q.K., C.M.M., R.V., S.L., S.N.S., K.M.I., A.G., R.P., N.R.C., C.S.H., A.H.Z., S.E.S., M.C.J., M.W., A.C.W., D.M.C., D.Z., Y.H., J.D.N., P.Z. and P.M. performed experiments and analyzed data. L.B., X.S., J.A.F. and J.A.Z. analyzed data. A.G.A., S.Q.K., C.M.M., R.V., S.L., L.B., S.E.S., M.C.J., X.S., G.G., E.M., M.N., J.A.F., K.Z., K.-H.C., M.S.S., C.J.W. and J.A.Z. wrote the paper.

Competing interests

All authors were employees and shareholders of Editas Medicine at the time the work was performed. J.A.Z. and C.M.M. are inventors on patent WO2021226151A2 that has been filed by Editas Medicine relating to this work.

Additional information

Supplementary information The online version contains supplementary material available at https://doi.org/10.1038/s41587-023-01779-8.

Correspondence and requests for materials should be addressed to John A. Zuris.

Peer review information *Nature Biotechnology* thanks Fyodor Urnov and the other, anonymous, reviewer(s) for their contribution to the peer review of this work.

nature research

Corresponding author(s): John Zuris

Last updated by author(s): Mar 28, 2023

Reporting Summary

Nature Research wishes to improve the reproducibility of the work that we publish. This form provides structure for consistency and transparency in reporting. For further information on Nature Research policies, see our Editorial Policies and the Editorial Policy Checklist.

Statistics

For all statistical analyses, confirm that the following items are present in the figure legend, table legend, main text, or Methods section.

n/a	Confirmed
☐	☒ The exact sample size (*n*) for each experimental group/condition, given as a discrete number and unit of measurement
☐	☒ A statement on whether measurements were taken from distinct samples or whether the same sample was measured repeatedly
☐	☒ The statistical test(s) used AND whether they are one- or two-sided *Only common tests should be described solely by name; describe more complex techniques in the Methods section.*
☒	☐ A description of all covariates tested
☐	☒ A description of any assumptions or corrections, such as tests of normality and adjustment for multiple comparisons
☐	☒ A full description of the statistical parameters including central tendency (e.g. means) or other basic estimates (e.g. regression coefficient) AND variation (e.g. standard deviation) or associated estimates of uncertainty (e.g. confidence intervals)
☒	☐ For null hypothesis testing, the test statistic (e.g. *F*, *t*, *r*) with confidence intervals, effect sizes, degrees of freedom and *P* value noted *Give P values as exact values whenever suitable.*
☒	☐ For Bayesian analysis, information on the choice of priors and Markov chain Monte Carlo settings
☒	☐ For hierarchical and complex designs, identification of the appropriate level for tests and full reporting of outcomes
☒	☐ Estimates of effect sizes (e.g. Cohen's *d*, Pearson's *r*), indicating how they were calculated

Our web collection on statistics for biologists contains articles on many of the points above.

Software and code

Policy information about availability of computer code

Data collection	Data collection for flow cytometry was performed using NovoCyte Quanteon (Agilent Technologies). Software used to acquire flow data was NovoExpress 1.5.6 (Agilent Technologies). Supporting graphical limages were generated using licensed Geneious Prime 2023.0 software, Microsoft Powerpoint software, and BioRender software, with additional graphic design support provided by Porterhouse Medical.
Data analysis	Graphing and statistical analysis was performed in GraphPad Prism (v9.5.1). All sequencing analysis was performed using publicly available tools as described in Methods section of manuscript. Flow cytometry data was analyzed using Flowjo (v10.8.1, Tree Star). Custom code used to analyze Digenome-Seq data is available at GitHub under the address https://github.com/editasmedicine/digenomitas. Custom code used to identify candidate in silico off-target sites is also available at GitHub under the address https://github.com/editasmedicine/calitas.

For manuscripts utilizing custom algorithms or software that are central to the research but not yet described in published literature, software must be made available to editors and reviewers. We strongly encourage code deposition in a community repository (e.g. GitHub). See the Nature Research guidelines for submitting code & software for further information.

Data

Policy information about availability of data

All manuscripts must include a data availability statement. This statement should provide the following information, where applicable:

- Accession codes, unique identifiers, or web links for publicly available datasets
- A list of figures that have associated raw data
- A description of any restrictions on data availability

Source data are provided with this paper. Unprocessed flow cytometry and microscopy images for Figures 1-5 is provided Source Data File 1 and numerical values for plotted data in Figures 1-5 is found in Source Data File 2. DNA constructs, guide RNAs, primers, ddPCR probes, Digenome-Seq results (SI Fig. 7a), rhAmp-Seq

panel of potential off-target candidate sites (SI Fig. 7b) are listed in Supplementary Table. All numerical data used in the generation of graphs in Supplementary Information Figures 1-18 are found in Supplementary Data. Raw flow cytometry plots and representative gating strategies, as well as uncropped microscopy and gel images, are provided in the Supplementary Information under Supplementary Notes. High-throughput sequencing data have been deposited in the NCBI Sequence Read Archive database (accession code: PRJNA947757) and found at this address http://www.ncbi.nlm.nih.gov/bioproject/947757.

Field-specific reporting

Please select the one below that is the best fit for your research. If you are not sure, read the appropriate sections before making your selection.

☒ Life sciences ☐ Behavioural & social sciences ☐ Ecological, evolutionary & environmental sciences

For a reference copy of the document with all sections, see nature.com/documents/nr-reporting-summary-flat.pdf

Life sciences study design

All studies must disclose on these points even when the disclosure is negative.

Sample size	Sample sizes were not predetermined based on statistical methods, but were chosen according to the standards of the field (at least three independent experiments). For flow cytometry, sample size was determined by acquiring 10,000 cells under the FSC vs SSC gate as this is standard practice in the field with the cell types investigated in this study. For most cases, biological triplicate experiments were performed unless otherwise noted.
Data exclusions	No data was excluded from analysis.
Replication	Results were replicated across multiple experiments as indicated in the figure legends. Number of biological replicates (usually n >= 3) are indicated in the figure legends. Replication of flow cytometry and next-gen sequencing editing data on genomic DNA extracted from cells was performed independently, as indicated in the relevant figures in the manuscript. All replication attempts were successful and averaged with statistics as appropriate.
Randomization	For the SKOV-3 mouse model, animals were randomized before treatment with unedited and SLEEK DKI iNKs and/or antibody. Specifically, NSG mice were inoculated intraperitoneally (IP) with 0.25–1.00 x 106 luciferase (luc)-expressing SKOV-3 cell line (SKOV-3-luc) ovarian tumor cells. Three days after tumor inoculation, mice were assessed for tumor engraftment using bioluminescent imaging (BLI) and randomized into groups with similar tumor burden (n=8/treatment group).
Blinding	Investigators were not blinded during data collection and analysis in animal studies as this was not needed for this type of procedure in the study. While investigators were not blinded, measures were taken to avoid intentional skewing of data. These measures included randomization of animals after tumor establishment to ensure that the tumor burden was equally represented in various groups prior to receiving treatments and tracking individual animal data points longitudinally, which were then reviewed by individuals who were not directly involved in the studies. Investigators were blinded during processing of biological samples for genomic DNA extraction and sequencing and when performing analysis of on-target alternative editing outcomes.

Reporting for specific materials, systems and methods

We require information from authors about some types of materials, experimental systems and methods used in many studies. Here, indicate whether each material, system or method listed is relevant to your study. If you are not sure if a list item applies to your research, read the appropriate section before selecting a response.

Materials & experimental systems

n/a	Involved in the study
☐	☒ Antibodies
☐	☒ Eukaryotic cell lines
☒	☐ Palaeontology and archaeology
☐	☒ Animals and other organisms
☒	☐ Human research participants
☒	☐ Clinical data
☒	☐ Dual use research of concern

Methods

n/a	Involved in the study
☒	☐ ChIP-seq
☐	☒ Flow cytometry
☒	☐ MRI-based neuroimaging

Antibodies

Antibodies used	Flow cytometry: APC anti-human HLA-A/B/C (BioLegend, Cat# 311402 Clone W6/3, 1:100 dilution), BV421 anti-human TCR-α/β (BioLegend, Cat# 306722, Clone IP26, 1:100 dilution), FITC-labeled human CD19 protein (Acro Biosystems, Cat# CD9-HF2H2, 1:100 dilution), PE anti-human HLA-E (BioLegend Cat# 342604, Clone 3D12, 1:100 dilution), PerCP/Cyanine5.5 anti-human CD16 (BioLegend, Cat# 302028, Clone: 3G8, 1:50 dilution), BV786 mouse anti-human CD215 (IL-15Rα) (BD Biosciences, Cat# 747699, Clone: JM7A4, 1:16 diltuion), PE/Dazzle 594 anti-human CD3 (BioLegend Cat# 300450, Clone UCHT1, 1:100 dilution), PE/Cyanine 7 anti-human CD19 (BioLegend

Cat# 363012, Clone SJ25C1, 1:100 dilution), biotinylated recombinant human EGFR protein (Sino Biological, Cat# 29662-H27B-B, 1:100 dilution), PE anti-human CD107a (BD Biosciences, Cat# 555801, Clone: H4A3, 1:40 dilution), and streptavidin-FITC (Biolegend, Cat#405201, 1:200 dilution).

Immunohistochemistry:

Primary rabbit anti-Her2 (Abcam, ab16662, 1:1000 dilution).

Western blot:

Rabbit polyclonal anti-beta-tubulin (Novus Biologicals, 1:5000 dilution), mouse monoclonal anti-GAPDH (Cell Signaling Technologies, 1:1000 dilution), secondary anti-mouse HRP (Invitrogen, 1:5000 dilution), goat anti-rabbit IgG, HRP (Invitrogen, 1:5000 dilution), rabbit monoclonal anti-CD16 (Cell Signaling Technologies, 1:1000 dilution), secondary goat anti-rabbit IgG, HRP (Invitrogen, 1:5000 dilution).

Validation

Validation for all antibodies are provided on manufacturer's websites for the specific applications (Flow cytometry, Immunohistochemistry, Western blot) and all of these antibodies have been reported on previously in numerous instances in the literature. Examples are provided on the manufacturer website showing positive and negative controls.

APC anti-human HLA-A/B/C (BioLegend Clone W6/3, 1:100 dilution), BV421 anti-human TCR-α/β (BioLegend Clone IP26, 1:100 dilution), streptavidin conjugated FITC (Biolegend, 1:200 dilution),PE anti-human HLA-E (Biolegend Clone 3D12, 1:100 dilution), PerCP/Cyanine5.5 anti-human CD16 (BioLegend, Clone: 3G8, 1:50 dilution), PE/Dazzle 594 anti-human CD3 (BioLegend Clone UCHT1, 1:100 dilution), and PE/Cyanine 7 anti-human CD19 (BioLegend Clone SJ25C1, 1:100 dilution). The above listed antibodies were all verified by BioLegend.

Biotinylated recombinant human EGFR protein (Sino Biological, 1:100 dilution), verified by Sino Biological.
FITC-labeled human CD19 protein (Acro Biosystems, 1:100 dilution), verified by Acro biosystems.
BV786 mouse anti-human CD215 (IL-15Rα) (BD Biosciences Clone: JM7A4, 1:16 dilution), verified by BD Biosciences

Primary rabbit anti-Her2 antibody (Abcam, ab16662, 1:1000 dilution), verified by Abcam.

Secondary anti-mouse HRP (Invitrogen, 1:5000 dilution), goat anti-rabbit IgG, HRP (Invitrogen, 1:5000 dilution) and secondary goat anti-rabbit IgG, HRP (Invitrogen, 1:5000 dilution), verified by Invitrogen.

Rabbit polyclonal anti-beta-tubulin (Novus Biologicals, 1:5000 dilution), verified by Novus Biologicals.

mouse monoclonal anti-GAPDH (Cell Signaling Technologies, 1:1000 dilution) and rabbit monoclonal anti-CD16 (Cell Signaling Technologies, 1:1000 dilution), verified by Cell Signaling Technologies.

Eukaryotic cell lines

Policy information about cell lines

Cell line source(s)	We obtained all human cell lines from ATCC, iPSCs were obtained from RUCDR Infinte Biologics. Raji cells were purchased from ATCC (CCL-86). NALM-6 cells were purchased from ATCC (CRL-3273). K-562 cells were purchased from ATCC (CCL-243). The human iPSC lines were purchased from RUCDR Infinite Biologics (Cell line ID: NH50191, Lot # R018360480, R018496431). For iNK in vitro and animal studies, the iPSC line was obtained from BlueRock Therapeutics.
Authentication	Cell lines were authenticated by the provider
Mycoplasma contamination	Cell lines were free of Mycoplasma contamination, as determined by MycoAlert™ Mycoplasma Detection Kit (Lonza)
Commonly misidentified lines (See ICLAC register)	N/A

Animals and other organisms

Policy information about studies involving animals; ARRIVE guidelines recommended for reporting animal research

Laboratory animals	Animal studies were performed in compliance with animal guidelines and protocols approved by the Institutional Animal Care and Use Committee at CRADL: CR-0058. Six weeks old female non-obese diabetic (NOD) severe combined immunodeficient (SCID) gamma (NSG) mice were purchased from Jackson Laboratories (NOD.Cy-Prkdcscid/J #005557 Bar Harbor, ME) and maintained in pathogen-free conditions at the Charles River Accelerator and Development Lab (CRADL, Cambridge, MA). Mice were housed under dark and light cycles of 12 hrs. The average temperature was 21 °C with fluctuations ranging from 20 °C to 26 °C. Relative humidity averaged 60% and did not exceed 70% or fall below 30%.
Wild animals	No wild animals were used in this study.
Field-collected samples	No field collected sampled were used in this study.
Ethics oversight	All studies involving animals were performed under an IACUC approved protocol. Animal studies were performed in compliance with animal guidelines and protocols approved by the Institutional Animal Care and Use Committee at CRADL: CR-0058.

Note that full information on the approval of the study protocol must also be provided in the manuscript.

Flow Cytometry

Plots

Confirm that:

☒ The axis labels state the marker and fluorochrome used (e.g. CD4-FITC).

☒ The axis scales are clearly visible. Include numbers along axes only for bottom left plot of group (a 'group' is an analysis of identical markers).

☒ All plots are contour plots with outliers or pseudocolor plots.

☒ A numerical value for number of cells or percentage (with statistics) is provided.

Methodology

Sample preparation	For flow cytometry, cells were harvested, washed with 1X DPBS and resuspended in 1X DPBS containing relevant antibodies. Cells were stained for 30 mins in the dark at 4C. Later, cells were washed before data acquisition. For EGFR CAR staining, cells were stained with biotinylated human recombinant EGFR protein for 30 mins followed by washing and re-staining with streptavidin-FITC for 10 mins, washed and then used for data acquisition
Instrument	Flow cytometry data was acquired using the NovoCyte Quanteon (Agilent Technologies)
Software	Flow cytometry data was acquired on NovoExpress 1.5.6 and data was analyzed using FlowJo (V10.7.1, Tree Star)
Cell population abundance	10,000 cells gathered under FSC/SSC live gate for all measurements which was then followed by subgating for relevant markers depending on experiment
Gating strategy	Cells were first gated FSC-A/SSC-A, followed by FSC-A/FSC-H for singlets and then subgated for relevant markers depending on those specific markers being assessed in each experiment. Boundaries for specific markers were drawn based on positive or negative controls

☒ Tick this box to confirm that a figure exemplifying the gating strategy is provided in the Supplementary Information.